

Alma Mater Studiorum Università di Bologna  
Archivio istituzionale della ricerca

Modeling the effects of substrate fluctuations on the maintenance rate in bioreactors with a probabilistic approach

This is the submitted version (pre peer-review, preprint) of the following publication:

*Published Version:*

Maluta F., Pigou M., Montante G., Morchain J. (2020). Modeling the effects of substrate fluctuations on the maintenance rate in bioreactors with a probabilistic approach. BIOCHEMICAL ENGINEERING JOURNAL, 157, 1-17 [10.1016/j.bej.2020.107536].

*Availability:*

This version is available at: <https://hdl.handle.net/11585/760810.3> since: 2020-06-03

*Published:*

DOI: <http://doi.org/10.1016/j.bej.2020.107536>

*Terms of use:*

Some rights reserved. The terms and conditions for the reuse of this version of the manuscript are specified in the publishing policy. For all terms of use and more information see the publisher's website.

This item was downloaded from IRIS Università di Bologna (<https://cris.unibo.it/>).  
When citing, please refer to the published version.

(Article begins on next page)

This is the final peer-reviewed accepted manuscript of:

**Francesco Maluta, Maxime Pigou, Giuseppina Montante, Jérôme Morchain, *Modeling the effects of substrate fluctuations on the maintenance rate in bioreactors with a probabilistic approach*, Biochemical Engineering Journal, Volume 157, 2020, 107536, ISSN 1369-703X,**

The final published version is available online at:  
<https://doi.org/10.1016/j.bej.2020.107536>

Rights / License:

The terms and conditions for the reuse of this version of the manuscript are specified in the publishing policy. For all terms of use and more information see the publisher's website.

*This item was downloaded from IRIS Università di Bologna (<https://cris.unibo.it/>)*

***When citing, please refer to the published version.***

# Modeling the effects of substrate fluctuations on the maintenance rate in bioreactors with a probabilistic approach

Francesco Maluta<sup>a</sup>, Maxime Pigou<sup>b</sup>, Guiseppina Montante<sup>c</sup>, Jérôme Morchain<sup>d</sup>

<sup>a</sup>*Dipartimento di Ingegneria Civile, Chimica, Ambientale e dei Materiali, Alma Mater Studiorum – Università di Bologna, via Terracini 34, 40131 Bologna, Italy*

<sup>b</sup>*IMFT, allée du professeur Camille Soula, Toulouse*

<sup>c</sup>*Dipartimento di Chimica Industriale ‘Toso Montanari’, Alma Mater Studiorum – Università di Bologna, via Terracini 34, 40131 Bologna, Italy*

<sup>d</sup>*TBI, Université de Toulouse, CNRS, INRA, INSA, 135 Avenue de Rangueil, 31077 Toulouse, France*

---

## Abstract

A simple Interaction by Exchange with the Mean (IEM) mixing model is implemented to describe the glucose concentration segregations in industrial and laboratory scale bioreactors. This approach is coupled with a Population Balance Model (PBM) for the growth rate adaptation and a metabolic model dependent on the individuals state, both from the literature [1]. The model formulation is validated against different published experiments and it is shown that the IEM model reduces the computational costs when just the segregation of few species is of interest. A model for the maintenance costs of *Escherichia coli* subject to glucose concentration fluctuation is also presented and implemented in the context of the IEM mixing model. An Eulerian formulation of the effects of the substrate fluctuations on the maintenance rate is proposed and tied to a more intuitive Lagrangian vision. The study of these metabolic changes due to substrate heterogeneities helps the understanding of the relationships between hydrodynamics and cells metabolism and it improves the agreement between numerical and experimental data.

*Keywords:*

IEM, Mixing model, Substrate fluctuations, Maintenance rate, Bioreactors simulations, Metabolism

---

## 1. Introduction

The effect of mixing on bioreactions has been identified many years ago by Hansford and Humphrey [2]. Cultivating yeast in a continuous fermenter, these pioneers observed that the number and location of the injection points influence the glucose into biomass conversion yield.

The highest yields were observed when multiple injection points located in the vicinity of the impeller were used. Dunlop and Ye [3] observed that the biomass dry weight in a continuous fermenter increases when glucose is fed through an inlet port characterized by a smaller Kolmogorov length scale. In other words, well-micromixed bioreactors allow higher yields whereas poorly micromixed devices lead to lower yields and favour by-product formation. It is remarkable that these conclusions perfectly match the modern vision of the interaction between reaction and mixing developed by Bourne, Bałdyga and Villiermaux, among others, in the 80's [4, 5, 6]. The basic explanation is that mixing precedes the reaction. Since these two processes occur in series, the apparent rate of a chemical reaction as well as the formation of by-products are controlled by the rate of (turbulent) mixing. Following the microbiological explanation proposed by Hansford and Humphrey [2], Ye and Dunlop explained that *cells which encountered region of high sugar concentration diverted [...] a greater proportion of substrate carbon into extracellular product via endogenous metabolism* [7]. Thus, it appears that the substrate concentration distribution in a bioreactor impacts the yields as well as the rates of biochemical reactions. On the other hand, the interaction between mixing and bioreactions is more complex than in chemical reactors due to additional metabolic pathways triggered by repeated exposure to high and low concentrations (e.g. overflow metabolism for *Escherichia coli* or short-term Crabtree effect for yeasts). Nowadays, the commonly accepted idea regarding the effect of concentration heterogeneities is that they induce the activation of a large number of genes which causes an increase in the energy demand for maintenance as well as various metabolic responses, one of them being the formation of undesired by-products [8, 9, 10, 11]. In order to investigate these effects, several lab scale experimental devices, reviewed by Neubauer and Junne [12], were used to mimic the fluctuating environment encountered by the cells along their trajectory in an imperfectly mixed bioreactor [13, 14, 15, 16, 17]. Among these, the most popular device is a two-stage bioreactor, generally a Continuous Stirred Tank Reactor (STR) connected to a Plug Flow Reactor (PFR). Displacing the feed point in one or the other reactor allows creating a variety of configurations leading to distinct biological responses.

The interaction between mixing and bioreactions was also investigated by modelling methods. In the early 70's, a series of work from Tsai and co-workers investigated this question using the concepts of complete segregation and maximum mixedness [18, 19, 20]. In the work of Bajpai and Reuss, some refinements were introduced to account for the circulation time dis-

tribution [21]. However, these authors considered an unstructured kinetic model for bioreaction that basically assumes that bioreaction rates are determined from local concentrations using constant biological parameters. Clearly, kinetic or metabolic structured models are mandatory for they introduce internal variables, linked to the biotic phase, which dynamically adapt to the external environment. Thus, bioreactions rate may now depend on the cell state also. Quite naturally, it appears necessary to consider some diversity among a population of living cells. This can be achieved using either probability density functions, PDF, (leading to continuous Population Balance Equations, PBE) [22, 23, 24] or discrete formulations (cell based models along with Monte Carlo techniques to deal with large cell ensembles ) [25, 26, 27].

Beside the description of the biological phase, one has to consider the heterogeneity of the concentration field. The trend, in the last decades was to rely upon Computational Fluid Dynamics [28, 29, 30] or Compartment Model Approach to do so [31, 1, 32, 33, 34, 35]. In both cases, the spatial distribution of concentration is assessed. This knowledge, complemented with a Lagrangian particle tracking, can produce a temporal signal that is used as the boundary condition for a biological model (generally a set of ordinary differential equations) [36, 37, 38]. Thus, the effect of concentration fluctuations on the rate of biological reactions is obtained but the reverse coupling (modification of the concentration field due to bioreactions) is computationally very demanding and results are sensitive to the interaction of numerical parameters which makes such simulations unstable in their predictions. However, in order to address the subject of interest here, i.e. the interaction between mixing and bioreaction, a full two-way coupling is necessary. This requires the transport of the biological phase in the three-dimensional space of the bioreactor. This is possible using a Eulerian description for the biological phase (transport of PDF) but the number of biological variables in the model is then limited [1, 35]. So, the general trend is an ever-growing complexity, associated to a high level of expertise and prohibitively large numerical costs, which make these modelling tools inaccessible for industrial applications since the effort is not producing significant added value.

In this work, we investigate the possibility to rely upon the statistical description of the concentration distribution only, disregarding the spatial dimensions. A popular model of this type is the Interaction by Exchange with the Mean model (IEM) originally introduced by Villermaux to address micromixing issues [39]. In such models, the reacting volume is divided into two or more environments (or zones) and a characteristic time relative to mass exchange between

the zones is introduced. Considering only two environments suggests that the concentration distribution will be approximated by two Delta functions. It was shown that this can constitute a fair approximation of the actual concentration PDF in the limit of fast reactions. In fed-batch bioreactors, the characteristic time of substrate uptake generally decreases with time and becomes much smaller than the macromixing time [1, 40]. Hence, a fed-batch fermenter subject to mixing issue is usually strongly segregated and exhibits a highly concentrated zone near the feed point and a very low concentration zone elsewhere.

Considering the various time scales of the biological response to concentration fluctuations, we developed and validated the idea that the disequilibrium between the uptake and utilization rates provides a good estimate of the flux of substrate that must be diverted into by-products [30, 1]. However, up to now, the metabolic rate calculations assumed a growth rate dependent yield (namely a Pirt's law [41]) along with a constant maintenance rate. The idea of tying the maintenance rate to the process variables was already suggested by Holms [42] and by Meadows et al. [43], although they linked the maintenance rate to the growth rate. Since substrate fluctuations are known to produce a metabolic stress on bacteria and thus contribute to increasing the cells energy demand, it is proposed to relate the maintenance rate to the variance of the glucose concentration distribution. This rate dynamically updates the substrate into biomass yield, introducing in the model a coupling between the degree of mixing in the bioreactor and the glucose conversion efficiency.

This article presents the formulation of a segregation dependent maintenance rate. The Interaction by Exchange with the Mean (IEM) model is implemented in ADENON, an in-house developed bioreactor simulation software combining CMA, kinetic or mode based metabolic model and PBE approaches. Simulations results using the IEM model will be compared to the experimental observations published by Xu et al. [44] in a 20  $m^3$  reactor and by Neubauer et al. [16] in a STR+PFR scale-down reactor. Spatially refined simulation using CMA [1] (for the Xu experiment) and a two-stage STR+PFR (for the Neubauer experiment) are also performed to serve as references. The challenges posed by the two sets of experiments considered in this work are related to the presence of spatial inhomogeneities or segregation that trigger a suboptimal operation of the fermentation process. In the Xu et al. [44] experiment, the segregation is entirely due to the large scale of the reactor and the injection conditions that result in a poorly meso-mixed process. On the contrary, in the Neubauer et al. [16] experiment,

a segregated environment was intentionally designed by means of a multi-stage reactor, with localized injections.

In the final part of this work, some details are given regarding the formulation of an Eulerian expression of the maintenance rate starting from a Lagrangian perspective. It is shown that one can reconcile the Lagrangian and Eulerian visions of the biological response to external fluctuations.

## 2. The experiments

In this work two different sets of experiments found in the literature were simulated, one studying a fed-batch culture in an industrial scale bioreactor, described by Xu et al. [44] and lately simulated by Vrabel et al. [31] and Pigou and Morchain [1], and one by Neubauer et al. [16] dealing with a fed-batch culture in a pilot scale bioreactor.

Xu et al. [44] investigated the acetate production in an industrial scale fed-batch bioreactor with *E. coli*. The fermentation was performed in a  $20m^3$  stirred tank reactor equipped with Rushton impellers. The initial concentration of glucose was equal to  $0.29g_G/L$ , the initial concentration of acetate was equal to zero and the initial biomass concentration was  $X(t = 0) = 0.1g_X/L$ . After an initial batch phase of  $0.92h$ , a feed solution of glucose ( $454g_G/L$ ) was injected well above the upper impeller at variable flow rate with an exponential curve for  $8.5h$ , changed to a constant value of  $180L/h$  for  $2.5h$  and then to  $170L/h$  for  $28.02h$ . The sampling of glucose, acetate and biomass concentration was performed at three different sampling points located at the top, in the middle and at the bottom of the reactor. Glucose gradients were identified as the result of insufficient mixing. Acetate was produced in the upper part of the reactor and a reduction of the glucose to biomass yield of 25 % was observed with respect to the homogeneous 20L fermenter. This experimental observation could not be reproduced by Vrabel et al. but was correctly predicted by Pigou and Morchain owing to the use of a Pirt's law with a maintenance rate equal to  $0.250mmol_G \cdot g_X^{-1} \cdot h^{-1}$  ( $45mg_G \cdot g_X^{-1} \cdot h^{-1}$ ).

Neubauer et al. [16] investigated the *E. coli* responses to substrate fluctuations in a two-stages bioreactor of  $10L$  consisting in a closed loop of a STR connected to a PFR of  $0.695L$ , Fig.1. The initial glucose concentration was  $10g_G/L$  and the system was operated in batch to the complete depletion of glucose ( $\sim 8h$ ). Once completed the batch phase, the system was operated in fed-batch for  $8h$ , with the injection of glucose-rich solution ( $600g_G/L$ ) at a

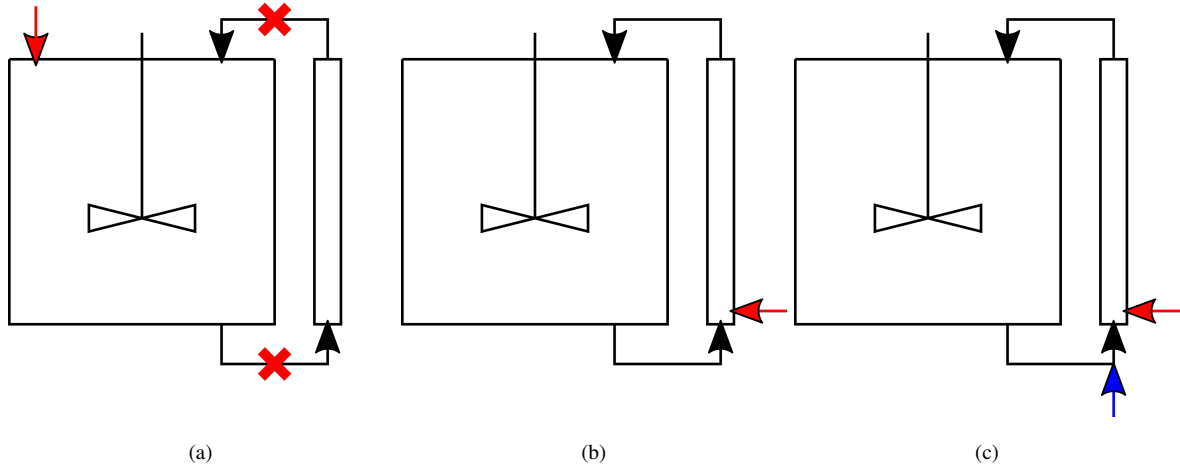


Figure 1: Schemes of the reactor configurations used in the Neubauer et al. [16] experiment: (a) injection of substrate (red arrow) in the STR operated without the PFR loop, *Case A*, (b) STR+PFR with injection in the PFR, *Case B1*, (c) STR+PFR with substrate injection in the PFR and aeration with oxygen enriched air (blue arrow), *Case B2*.

constant flow rate of  $50\text{ml}/h$  either in the STR or just before the PFR. The fed-batch results were collected for three different configurations: without the external PFR loop and injection in the STR (referred to as *Case A* or *Control*, in the publication, Fig.1a) and with the external loop and injection in the PFR (referred to as *Case B* in the publication, Fig.1b). The authors also investigated the use of oxygen enriched air as aeration gas in the PFR ( Fig.1c) to test the hypothesis that microaerobiosis would develop due to high substrate uptake. In the following we will refer to *Case B* configuration aerated with air as *Case B1*, Fig.1b, and to the same configuration aerated with oxygen enriched air as *Case B2*, Fig.1c. In each *Case*, the medium volume was kept constant to  $10L$ . The biomass concentration and growth rate as well as the glucose and acetate profiles in the PFR, were monitored in the Neubauer et al. [16] experiment. The residence time was  $113s$  for the PFR,  $\tau_{PFR}$ , and  $27min$  for the STR,  $\tau_{STR}$ . It was observed that the repeated exposure to high glucose concentration in the PFR, interrupted by prolonged periods of glucose limitation in the STR, led to an over-assimilation of glucose at the PFR inlet coupled with acetate production due to overflow metabolism and a reduced glucose to biomass yield in comparison to the homogeneous *Case A*. Some acetate was also produced in the upper part of the PFR because of oxygen limitation (fermentative catabolism). The addition of enriched air, *Case B2*, did not change the initial response at the PFR inlet but led to a lower formation of acetate in the upper part and a yield similar to that observed in case *Case A*. As



146 far as the authors know, these experimental results have not been simulated to date.

### 147 **3. Mathematical model**

#### 148 *3.1. General aspects*

149 A detailed explanation of the population balance model and the metabolic model formula-  
150 tions, the solution strategies and their implementation in ADENON were already published in  
151 previous works [1, 30, 45, 40]. However they are briefly outlined here to allow a clear iden-  
152 tification of the novelties provided in this work. The mass balance equation for a generic  $k$   
153 component in a generic homogeneous control volume,  $V$ , reads:

$$\frac{dC_k}{dt} = \frac{1}{V} \left( \int_{\Omega} C_k^{in} |v|^{in} \cdot d\omega - \int_{\Omega} C_k |v|^{out} \cdot d\omega \right) + R_k \quad (1)$$

154

155 where  $C_k$  is the concentration,  $\Omega$  is the surface enveloping the control volume,  $|v|^{in}$  and  
156  $|v|^{out}$  are the norms of the velocity vector entering and exiting the control volume, respectively,  
157 and  $R_k$  is the volumetric reaction rate. Velocities in Eq.1 come out from the solution of a  
158 hydrodynamic model. The Compartment Model Approach (CMA) falls into this category and  
159 the fluxes are calculated either from general considerations on the fluid dynamics of the system  
160 ([31, 1]) or retrieved from the CFD simulations ([32, 33, 34, 35]).

161 The microbial population is considered as segregated with respect to the specific growth  
162 rate  $\mu$ . Hence, the volumetric reaction rate in Eq.1 is expressed as an integral over the  $\mu$  space:

$$R_k = \int_0^{\infty} r_k(\mu, \mathbf{C}) X(\mu) d\mu \quad (2)$$

163

164 Where  $X(\mu)d\mu$  is the mass of cells able to grow at  $\mu$  per unit volume,  $r_k$  represents the net  
165 specific reaction rate and  $\mathbf{C}$  is the concentration vector of the species, considered as constant  
166 inside the generic homogeneous control volume  $V$ , as already assumed in the derivation of  
167 Eq. 1. The equation for the cell density function  $X(\mu)$  is obtained under the assumptions that  
168 daughter cells inherit the growth rate of their mother [46].

$$\frac{\partial X(\mu, t)}{\partial t} = -\frac{\partial}{\partial \mu} \left( X(\mu, t) \zeta(\mu) \right) + \mu X(\mu, t) \quad (3)$$

where the rate of change of  $X$  in the  $\mu$ -space,  $\zeta(\mu)$ , in its general form is:

$$\zeta(\mu) \propto \frac{1}{T^{u/d}} (\mu^* - \mu) \quad (4)$$

with  $T^{u/d}$  being a time constant which value depends on the direction of the rate of change of the specific growth rate and  $\mu^*$  being the growth rate at equilibrium that generally takes the form of a Monod equation. The adoption of a segregated model with the growth rate capability as the internal coordinate, Eq.3, was introduced to decouple the actual growth rate of the population from the local reactant concentrations, Eq.4. This decoupling introduces an *out-of-equilibrium* metabolic behaviour resulting in the production/depletion of by-products.

The net reaction rate  $r_k$  results from a call to a metabolic model that can be regarded as a function  $f$ .

$$(r_k, \mu^a) = f(\mu, C, Y_{k,l \neq k}) \quad (5)$$

The metabolic model adopted in this work corresponds to that already presented in [1] and combines mass and energy balances. It considers four categories of biological reactions namely the production of biomass through substrate and energy consumption (*Anabolism*), energy production either by means of an oxidative pathway (*Oxidative catabolism*) or by fermentation (*Fermentative catabolism*) and the production of acetate due to the overconsumption of glucose (*Overflow metabolism*) or fermentative metabolism. It is worth recalling here that acetate production takes place either if the energetic need for growth is not fulfilled through the oxidative pathway (acetate production through fermentation) or if a cell uptakes more glucose than the amount used in the anabolic reactions (acetate production through overflow metabolism). The essential feature of our metabolic approach is that the maximum value for the anabolic reaction rate is the cell property  $\mu$ . In a given environment some cells may be limited and some others not. Indeed, any limitation is actually relative to the cell state rather than defined in an absolute manner through concentration thresholds. In case of insufficient resources, the actual growth rate of some cells may be limited to  $\mu^a \leq \mu$ . The term  $r_k$  consists of a summation of the specific reaction rates for each of the aforementioned biological reaction, weighted by the corresponding stoichiometric coefficients. Among these coefficients, the substrate to biomass yield was up to now determined using the well known Pirt's law [41], Eq.6, leading to a growth-dependent glucose to biomass yield,  $Y_{XG}(\mu_j^a, m)$ .

$$\frac{1}{Y_{XG}(\mu_j^a, m)} = \frac{m}{\mu_j^a} + \frac{1}{Y_{XG}^{max}} \quad (6)$$

In Eq.6,  $Y_{XG}^{max}$  is the maximum conversion yield of glucose into biomass,  $m$  is the maintenance rate (treated as a constant) and  $\mu^a$  is the actual growth rate of the cell.

### 3.2. New considerations

#### 3.2.1. Effect of substrate fluctuation on the maintenance rate

Having in mind the effects of imperfect mixing on cell physiology mentioned in the introduction, it is proposed to introduce a variable maintenance rate and express it as a function of the variance of the substrate concentration distribution in the system.

$$\bar{m} = m_0 + \alpha \int p(C_G) (C_G - \langle C_G \rangle)^2 dC_G \quad (7)$$

where  $m_0$  is the minimum maintenance rate of the cells,  $\alpha$  is the model parameter,  $C_G$  is the substrate concentration,  $\langle C_G \rangle$  is the volume average of the substrate concentration in the fermenter and  $p(C_G)dC_G$  is the volume fraction of the reactor with a concentration  $C_G$ . Hypothesizing that the cells are uniformly distributed inside the reactor volume and dividing the reactor into  $N_C$  sub-volumes of equal size a discrete expression can be formulated :

$$\bar{m} = m_0 + \alpha \frac{1}{N_C} \sum_{i=1}^{N_C} (C_{G,i} - \langle C_G \rangle)^2 \quad (8)$$

Eq.8 provides an Eulerian integral correlation between the sub-volumes concentration deviation from the volumetric average in the whole reactor and the average maintenance rate of any cell travelling in an heterogeneous concentration field. The derivation of Eq.8 from the effects of substrate fluctuations on a single cell and on a swarm of Lagrangian cells is described in Section 6.2.

#### 3.2.2. The Interaction by Exchange with the Mean Mixing Model

In the IEM approach, the composition space of the species is discretized rather than the physical space of the reactor. The space of composition can be divided into two or more environments, Fig.2b, that interact due to mixing. In the experiments presented, the bioreactors are strongly segregated and a description of the concentration distribution based on two environments (with high and low substrate concentration) constitutes a reasonable approximation.

Let us consider a generic concentration distribution inside a reactor during a fed-batch fermentation, Fig.2a. In this distribution it is possible to encounter two different peaks, one at a lower

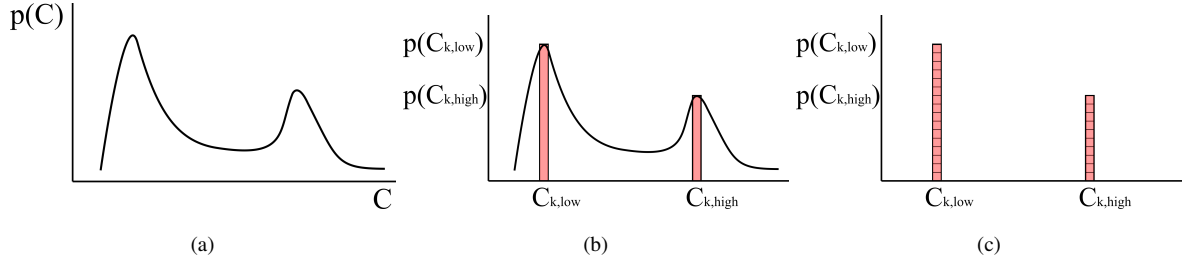


Figure 2: Hypothesized concentration distribution in a fed-batch reactor (a), its description by means of two environments (b) and discretization through elementary probability units (c).

concentration,  $C_{k,low}$ , with a higher probability,  $p(C_{k,low})$ , and one at a higher concentration,  $C_{k,high}$ , with a lower probability,  $p(C_{k,high})$ , corresponding to the bulk of the reactor and the poorly meso-mixed region in the vicinity of the species injection, respectively. The interaction of the species compositions in the different environments occurs by means of a mixing model [47].

The environments can be discretized in a number of elementary probability units, Fig.2c, that can be thought as presumed sub-volumes in case the environments probabilities remain constant in time. A fundamental assumption in the IEM model is that each elementary sub-volume has the same probability to exchange mass with each and every elementary sub-volume, including those of the same environment. Therefore, the results of these exchanges can be represented by a single exchange with a fictitious volume at the volume average concentration  $\langle C_k \rangle$ . The resulting equations for the segregated species are:

$$\frac{dC_{k,low}}{dt} = \frac{1}{\tau_m} (\langle C_k \rangle - C_{k,low}) + R_{k,low} \quad (9)$$

$$\frac{dC_{k,high}}{dt} = \frac{1}{\tau_m} (\langle C_k \rangle - C_{k,high}) + R_{k,high} + S_k \quad (10)$$

$S_k$  is a source term for the species under consideration representing the feed. The volume average concentration of any distributed species is computed as :

$$\langle C_k \rangle = p(C_{k,low})C_{k,low} + p(C_{k,high})C_{k,high} \quad (11)$$

Having described the inhomogeneities in the system in terms of concentration space segregation instead of physical space segregation, the term  $\tau_m$  is the only parameter of the model, related to some mixing time constant, which defines the rate of exchange between sub-volumes.

The IEM model distributes just the species that cannot be considered as homogeneously dispersed in the volume. The reaction rates are calculated in each sub-volume and the concentrations of the homogeneously dispersed species are then volume-averaged to retain just one value per species. The concentration of the homogeneously dispersed species is then a composition of all the concentrations in the sub-volumes (which change differently due to the different reaction rates), whereas the concentration of the distributed species is a vector with as many elements as the total number of sub-volumes.

### 3.3. Implementation in ADENON

All simulations were performed with ADENON, a simulation software developed in the MATLAB R2016a environment by this research group. The software focus is mostly directed at the simulation of bioreactors, by solving biological models within a fluid dynamics framework (compartment models, plug-flow reactors, stirred tank reactors, interconnected multi-stage reactors, batch or fed-batch cultures as well as accelerostat cultures). ADENON formulates a system of ODEs in terms of mass and volume balances, based on the user defined case configuration. This set of ODEs is then solved using the Runge-Kutta 2,3 explicit scheme for time integration.

In the previous section, two environments were considered. Dividing each of these environments into elementary subvolumes of the same size allows a direct calculation of the probabilities  $p(C_{k,low})$  and  $p(C_{k,high})$  as the ratio of the number of sub-volumes in each environment to the total number of sub-volumes.

$$p(C_{low}) = \frac{N_C^{low}}{N_C} \quad (12a)$$

$$p(C_{high}) = \frac{N_C^{high}}{N_C} \quad (12b)$$

In this work we hypothesized that the environment probabilities remain constant during the fermentation.

Each environment being made of a collection of identical elementary sub-volumes, the average concentration now writes :

$$\langle C_k \rangle = \frac{1}{N_C} \sum_{i=1}^{N_C} C_{k,i} \quad (13)$$

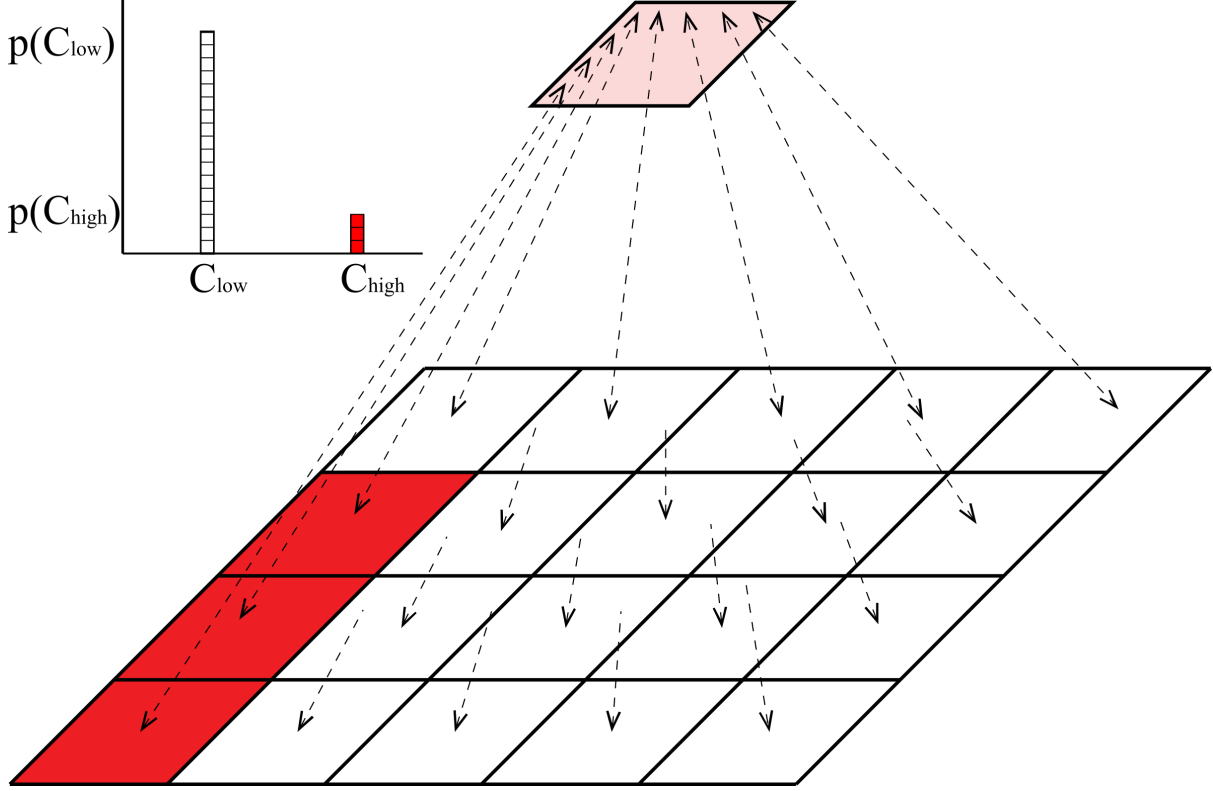


Figure 3: Scheme of an Interaction by Exchange with the Mean model. The scheme represents the two environments made of a collection of sub-volumes that exchange with their mean at the top. For any sub-volume, the sum of mass exchanged with the other sub-volumes is equivalent to a single exchange with a fictitious volume at the mean concentration. In the top left corner, the concentration distribution described by means of two environments discretized through elementary probability units.

The implementation of the IEM model in the framework a compartment based code is presented in Fig.3. As an illustration, the system consists of  $N_C = 20$  sub-volumes (the 20 squares composing the larger square) and two environments, corresponding to the fraction of the total volume at a given composition (represented by the total number of red,  $N_C^{high}$ , and the total number of white squares,  $N_C^{low}$ ). The arrows represent the exchange between each sub-volume and the mean. The corresponding environment distribution is represented as well. By changing the number of sub-volumes in which there is an injection,  $N_C^{high}$ , and the number of total sub-volumes,  $N_C$ , the probabilities of the environments with low and high concentration can be adjusted to any experimental configuration. It is of practical interest to consider a

collection of sub-volumes in the view of implementing the IEM model in the framework of a multi-compartment based simulator. At first sight, solving  $N_C$  equations instead of two looks like a waste of time, a step back due to the code structure. However, the benefit is that all simulations presented in this work, irrespective of the hydrodynamic model (CMA or IEM), are performed under the same modeling framework, using the same models for population and metabolic aspects of the problem.

## 4. Simulation set-up

### 4.1. Large scale Fed-Batch

The  $20m^3$  fed-batch experiment was simulated using the CMA with 70 compartments (as in [1] and [31]) in order to assess the IEM model against it. The initial conditions of the simulation were set to replicate the experiment and the initial biomass concentration was initialized at  $\mu(t=0) = 0.63h^{-1}$ . The authors reported that “*the dissolved oxygen signal did not show any oxygen limitation*” but hypothesized that the acid production was due to high substrate concentration inducing local oxygen limitations. Simulation due to Pigou and Morchain [1] showed that the acetic acid was indeed produced through the overflow metabolism rather than through fermentative pathways. Consequently, the oxygen inter-phase mass transfer rate was neglected and the concentration of the dissolved oxygen in the liquid was always considered at saturation ( $\sim 10mg_O/L$ ). The general situation where both sugar and oxygen gradients are present is not covered here. It certainly raises new challenges and some considerations are proposed at the end of the discussion part.

In our IEM simulation, the injection occurred in 1 of 70 sub-volumes, in the same way as Vrabel et al. [31] and Pigou and Morchain [1] did in the context of a compartment model. Simulating the Xu et al. [44] mixing time experiment with the IEM model allows the identification of  $\tau_m$  leading to the same macromixing time of 250s, Fig.4. The IEM model, of course, loses the spatial information regarding the tracer concentration, but, using an IEM model parameter equal to  $\tau_m = 36s$ , it is able to reproduce the macromixing time.

In Fig.4 the evolution of the tracer concentration at the three monitored locations as predicted by Pigou and Morchain [1] is shown. The macromixing time is calculated as the time needed by the tracer to reach a concentration of  $\pm 5\%$  of the final concentration and Fig.4 shows that the non-dimensional concentration at the bottom probe reaches the  $\pm 5\%$  interval

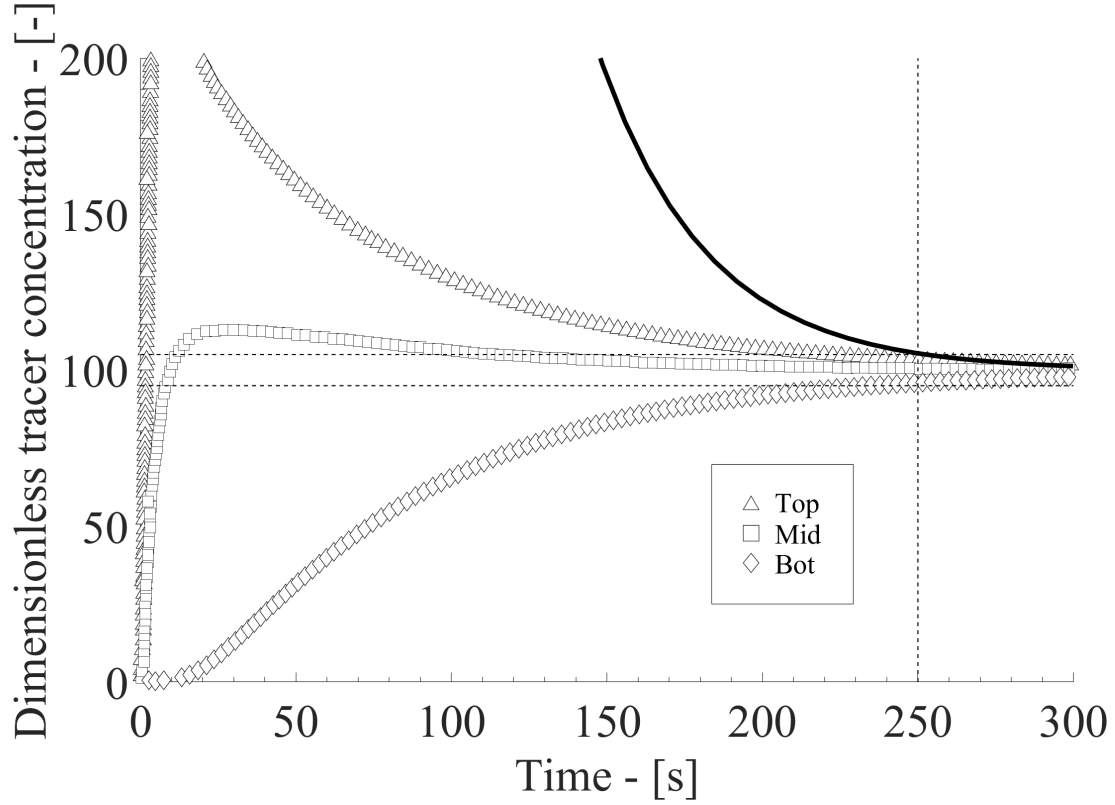


Figure 4: The open symbols represent the passive tracer evolution in time at the top (*top*), middle (*mid*) and bottom (*bot*) of the fermenter as predicted by Pigou and Morchain [1] with the CMA. The tracer evolution in time as predicted by the IEM is plotted with the solid line and the mixing time of 250s is highlighted by the dashed line.

after  $\sim 250s$ .

#### 4.2. Two stage bioreactor STR+PFR

Considering the Neubauer et al. [16] experiment, the reference case is a spatially refined simulation performed considering a STR connected to a PFR. The initial conditions were set to replicate the experiments and the initial biomass concentration was initialized at  $\mu(t=0) = 0.65h^{-1}$ . When the IEM model is used, the biomass, the acetate and the oxygen were treated as perfectly mixed species. In both cases, the oxygen inter-phase mass transfer rate was neglected considering the concentration of the dissolved oxygen in the liquid always at saturation ( $\sim 10mg_O/L$ ). This condition, according to the authors, would be valid for most of their experimentally characterized reactor configurations. The injection being located in the PFR, Fig.5a, this configuration resembles a poorly mesomixed fed-batch in a stirred tank reactor in which the injection plume is segregated from the bulk of the volume and the fresh



substrate has to travel the whole length of the jet before being released in the bulk (zone model), Fig.5b.

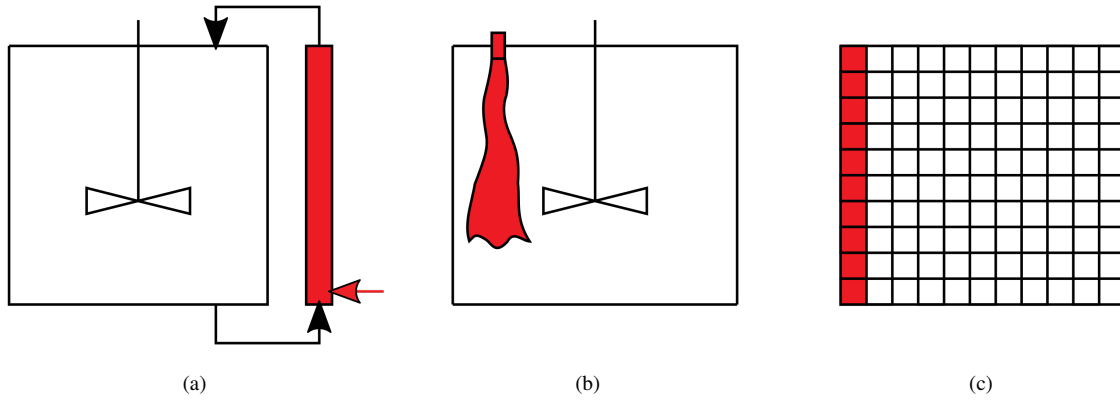


Figure 5: Reactor configuration of *Case B* in the Neubauer et al. [16] experiment (a). Poorly mesomixed fed-batch in a stirred tank reactor (b) and its description by means of the IEM model (c).

The IEM model, Fig.5c, further simplifies the system dropping the spatial information. The model only deals with the two environments, the plume and the bulk with high and low substrate concentration respectively and assumes that the characteristic interaction time between these two environments is equal to the PFR residence time, equal to 113s, therefore this time was chosen for  $\tau_m$ . A total number of 187 sub-volumes was defined in the simulations and the injection in the PFR was reproduced through a source term in 13 sub-volumes, obtaining a ratio of  $13/187 = 0.0695$  that closely matches the ratio between the experimental volumes  $0.695L/10L = 0.0695$ .

### 4.3. Biological constants

All simulations are performed using the same metabolic model. A detailed presentation of the model can be found in [1] (Appendix A). The same notations are used in this work. In that previous study, the constants for the Xu et al. [44] experiment were determined and their values are used in this work. The constants of the Neubauer et al. [16] experiment were tuned to match the homogeneous *Case A* results. A sensitivity analysis was performed on the most influential constants shown in Tab.1 and it is reported in Appendix A. The constants that have the highest influence on the results of the simulations considered in this work are:

- $\phi_O^{max}$ , the maximum oxygen uptake rate;
- $K_{i,A}$ , the acetate inhibition constant (in the expression of growth on glucose);

- $K_{i,A}^o$ , the acetate inhibition constant (in the oxygen uptake rate);
- $m$ , the maintenance rate (see Eq.6);
- $Y_{AG}$ , the glucose to acetate conversion yield (see Eq.5);
- $Y_{XG}^{max}$ , the maximum glucose to biomass conversion yield (see Eq.6).

The constant values for the two sets of simulations are reported in Tab.1.

Table 1: Model constants and their values used to simulate the Xu et al.[44] experiment and the *Case A* of the Neubauer et al. [16] experiment.

Constant	Xu et al. [44]	Neubauer et al. [16]	Units
$\phi_O^{max}$	15.60	14.00	$mmol_O/g_X \cdot h$
$K_{i,A}$	3.00	3.50	$g_A/L$
$K_{i,A}^o$	3.00	3.00	$g_A/L$
$m$	0.250	0.150	$mmol_G/g_X \cdot h$
$*Y_{AG}^{ferm}$	3.00	3.00	$mol_A/mol_G$
$*Y_{AG}^{over}$		2.00	$mol_A/mol_G$
$Y_{XG}^{max}$	1.32	1.50	$mol_X/mol_G$

\*The conversion yield of glucose in acetate in the Neubauer et al. [16] experiment was divided depending on the acetate production mechanism, i.e. fermentation (ferm) and overflow (over)

Although  $Y_{XG}^{max}$  is slightly different, the impact on simulated results is moderate due to the dominating role of maintenance,  $m$ , in equation Eq.6

## 5. Results

In this Section the results obtained with the IEM model in the two experimental set-ups described in Section 2 are shown and compared with the experimental data and the results from the compartment model [1]. Results obtained considering the reactor as perfectly homogeneous are shown as well. The dimensions of the spaces used in the simulations of the experiments are presented in Tab.2. The first set of results corresponds to a constant maintenance rate, the second set is obtained with a variable maintenance rate.

Table 2: Dimensions of the spaces used in the simulations.

	Physical space	$\mu$ space	$C$ space
Homogeneous model	0	1	0
Compartment model	3	1	0
IEM model	0	1	1

### 5.1. Constant maintenance rate

#### 5.1.1. Simulating the Xu experiment

Fig.6 shows the average biomass, the glucose and the acetate concentration time evolution obtained with a maintenance rate equal to  $0.250 \text{ mmol}_G / g_X \cdot h$ .

Concerning the average biomass concentration, Fig.6a, all the three modeling strategies achieve a satisfactorily agreement with the experimental data. Taking into account spatial heterogeneities and biological diversity is not critical in predicting the total biomass. Indeed, the total amount of biomass is essentially driven by the substrate feed rate and the substrate into biomass conversion yield. Minor differences in the biomass concentrations are however observed because different amounts of acetate are produced and re-consumed depending on the fact that substrate heterogeneity is described or not. In Fig.6b, the evolution of the substrate concentration is reported. The glucose concentration profiles of the IEM, compartment and even the homogeneous case up to  $\sim 7h$  perfectly overlap. As the spatial inhomogeneities become more important, three trends appear in the compartment model, depending on the sampling position. This aspect is overlooked by the IEM model, nonetheless, it produces results that are the same order of magnitude as the compartment model results and the use of this simplified model does not worsen the agreement with the experimental data, with respect to the more accurate compartment model. Fig.6c shows the time evolution of the concentration of acetate. IEM and compartment model results are in good agreement up to  $\sim 8h$  and, as for the data in Fig.6b, the agreement between experimental and numerical concentration profile as predicted by the compartment and IEM model does not change appreciably. Considering the system as perfectly mixed, on the other hand, lead to an underestimation of the acetate concentration that is identically zero between  $9h$  and  $32h$  from the beginning of the process. This latter result is in line with the fact that acetate is produced by overflow metabolism which

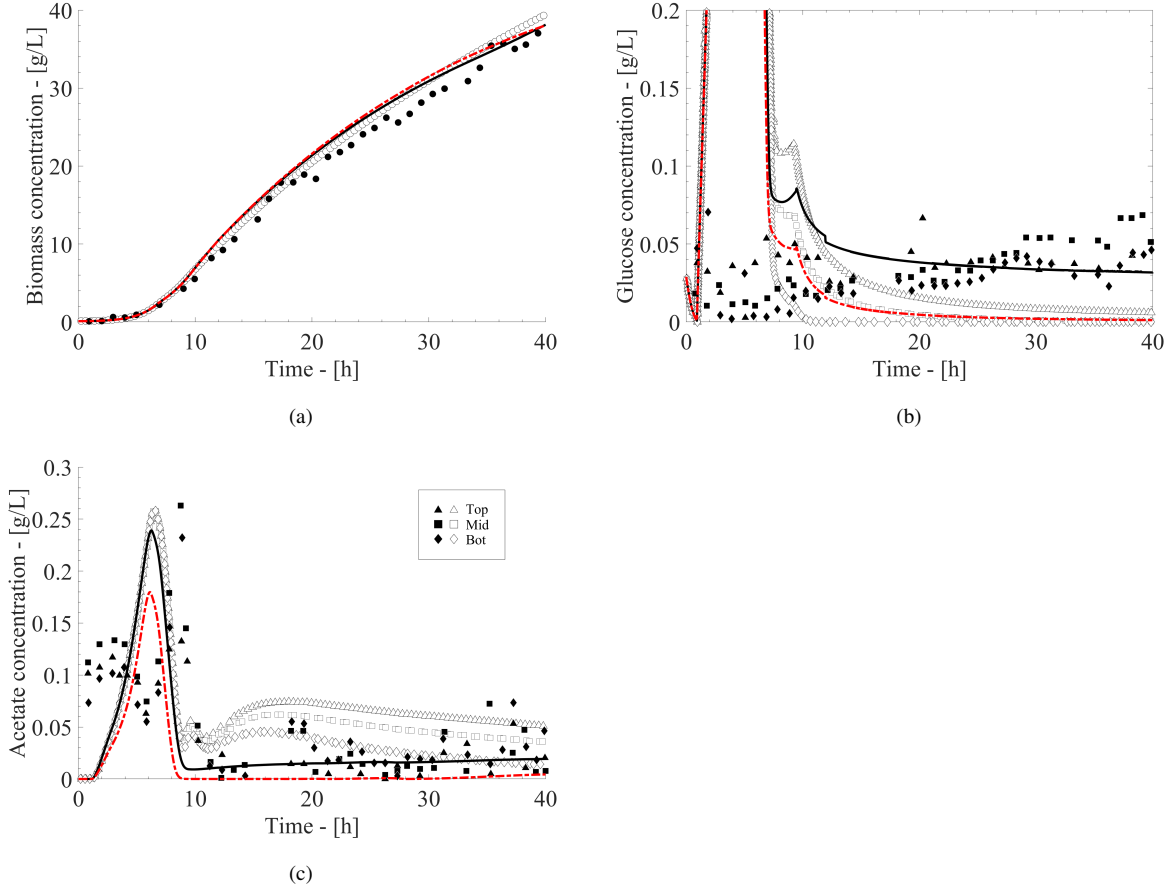


Figure 6: Average Biomass (a), Glucose (b) and Acetate (c) concentration evolution in the Xu et al. [44] experiment. Experimental data (filled symbols) and Compartment model results (open symbols) are collected at the top (*top*), middle (*mid*) and bottom (*bot*) of the fermenter, IEM model results (solid line), Homogeneous model (dashed line). All the numerical data are obtained with  $\bar{m} = 0.250 \text{ mmol}_G / \text{g}_X \cdot \text{h}$ .

results from the cell exposure to concentration heterogeneities only.

The results obtained from the numerical simulation of the Xu et al. [44] experiment show that the IEM model produces results that are in substantial agreement with the averaged global experimental data, while the homogeneous model results deviate appreciably but not significantly from the IEM and compartment models, with the largest differences found in the production of acetate. This latter result confirms that acetate is produced through overflow metabolism. In the model, this metabolic response is due to the local disequilibrium between uptake and growth rates. Therefore, the distribution of glucose must be considered, either from a spatial point of view (CMA) or a statistical point of view (IEM), to account for by-product formation.

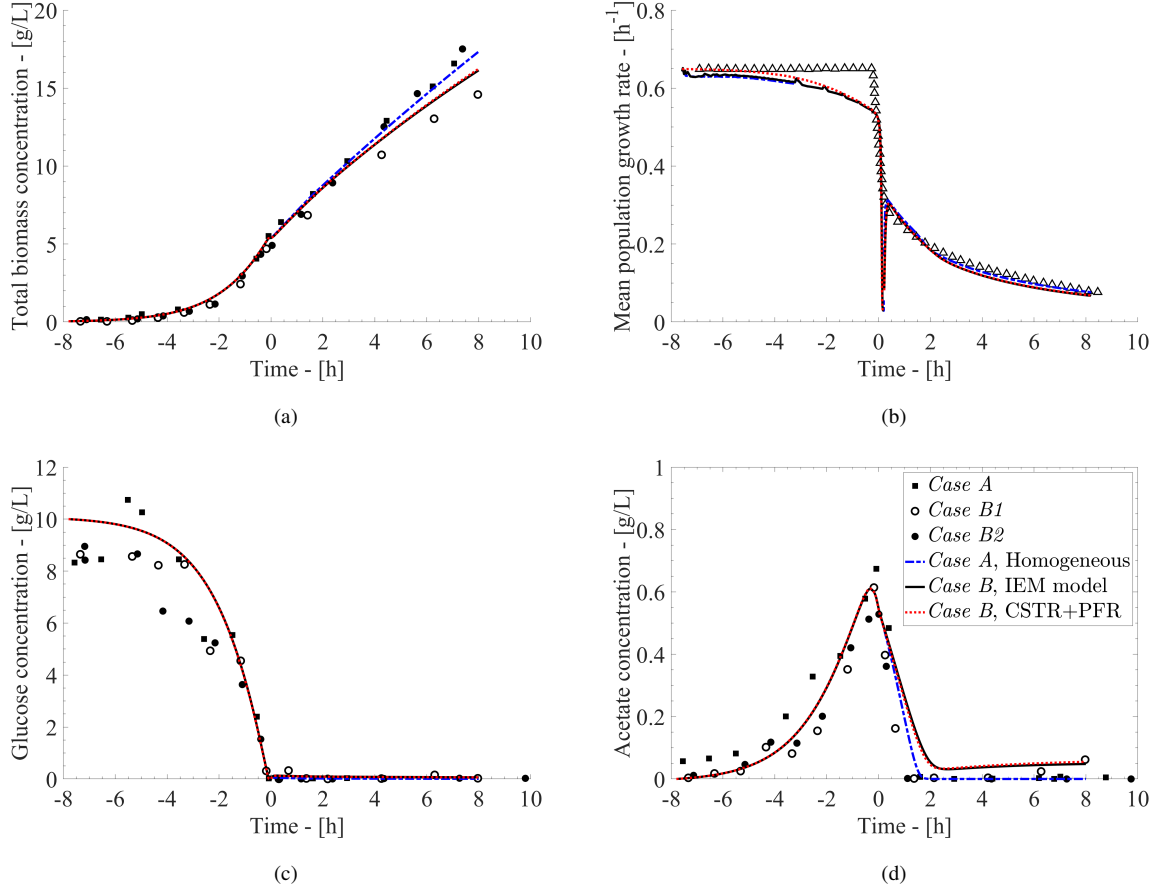


Figure 7: Biomass (a), Growth rate (b), Glucose (c) and Acetate (d) concentration evolution in the Neubauer et al. [16] experiments. Experimental data of *Case A* (squares) and *B* (circles) are shown together with the results of the homogeneous simulations (dashed line), the STR+PFR model (dotted line) and the IEM model (solid line). All the numerical data are obtained with  $\bar{m} = 0.150 \text{ mmol}_G / g_X \cdot h$ .

### 5.1.2. Simulating the Neubauer experiment

The experimental results of Neubauer et al. [16] and the simulation results are shown in Fig. 7. Fig. 7a, shows the evolution of the biomass concentration in the bioreactor for the *Case A* and *Case B*. The single STR *Case A* is simulated using a homogeneous model, while the *Case B* is simulated using either a two-stage bioreactor (STR+PFR) or the IEM model. The constants of the metabolic model reported in Tab. 1 were tuned in order to reach an agreement between the perfectly mixed *Case A* and the homogeneous model. As explained in Appendix A, the most influential parameter are, with little surprise, the maintenance rate and the maximum glucose into biomass yield. Thanks to this tuning, the numerical results of the homogeneous model closely match the perfectly mixed experimental data. It is interesting to note that the constant maintenance rate is now equal to  $0.150 \text{ mmol}_G / g_X \cdot h$ , much lower than the value necessary to

simulate the highly segregated Fed-batch of Xu et al. Regarding the simulation of *Case B*, the biomass concentration profiles as predicted by the IEM and the STR+PFR models almost perfectly overlap, indicating that considering the biomass as perfectly mixed could be an acceptable hypothesis when examining integral results, even in this reactor configuration. The IEM and the STR+PFR model, on the other hand, both over-predict the amount of biomass produced in *Case B1* (open circles) during the fed-batch phase, although exhibiting a trend that qualitatively agrees with this experimental set-up, i.e. a non-linear reduced production of biomass in time.

The mean growth rate evolution in time is shown in Fig.7b, where a very good agreement between the experimental and numerical results is achieved throughout most of the process. Between  $t = -5h$  and  $t = 0$  a noticeable deviation between the numerical and experimental data occurs, but, considering the strongly non-linear biomass growth in the same time interval (Fig.7a), this deviation can be explained by the fact that a constant growth was hypothesized during the batch phase by the authors of the experiment.

Considering the glucose consumption dynamics, shown in Fig.7c, the overall trend and the quantitative agreement in the fermentation is very convincing. In the overall growth rate evolution and in the glucose consumption almost no differences exist between the homogeneous, the IEM and the STR+PFR models. Nonetheless, a deviation between experiments and simulations appears between the beginning of the process and  $\sim -3h$ . In Neubauer et al. [16], it is said that the culture medium used for the batch phase of the fermentation contained 10.0g of glucose per liter, whereas the experimental data are slightly lower. Therefore the misalignment between simulated and experimental data may be due to inaccuracies in the acquisition of the latter set of data.

Concerning the evolution of the acetate concentration, Fig.7d shows two distinct trends. The acetate produced during the batch phase is rapidly re-consumed when the residual concentration of glucose becomes low. During the fed-batch phase, no acetate is produced in the *Case A* whereas it accumulates when injection is performed in the PFR. As stated earlier in the description of experiments, acetate is produced through overflow metabolism when cells enter the PFR and face a high glucose concentration. It is also produced through fermentation at the end of the PFR because of oxygen limitation *case B1*. This second source of acetate production vanishes if enriched air is used in the PFR *Case B2*. In any case, acetate is also re-consumed in

the STR where the glucose concentration is low. These multiple sources of acetate production and re-consumption are taken into account in our metabolic model. In our simulations, the acetate in the homogeneous model is completely depleted after few hours from the beginning of the fresh substrate injection. This is a consequence of our metabolic model which considers that acetate is uptaken if the amount of glucose is insufficient to satisfy the cell needs for growth. The initial re-consumption also takes place in *Case B* and it is correctly represented by the IEM and the STR+PFR models. Moreover both models predict a remaining low but not negligible amount of acetate that is confirmed by the experimental data collected in the *Case BI* configuration.

The model predictions are consistent for glucose, acetate and growth rate but still some discrepancy remains regarding the calculation of the biomass concentration. One of the major unsolved aspects in the discussion presented above is the over-prediction of biomass in the *Case BI* of the Neubauer et al. [16] experiment. Neubauer et al. [16] report a reduction of the conversion yield of glucose in biomass,  $Y_{XG}$ , from 0.5 to 0.38  $g_X \cdot g_S$  (-25 % roughly). Similarly, Xu et al. [44] had to reduce by 25 % the value of  $Y_{XG}$  identified in an homogeneous lab scale reactor in order to fit their results in the heterogeneous large scale fed-batch bioreactor. As a matter of fact, despite the description of the spatial inhomogeneities in the reactor, a constant  $m$  value, fitted from the perfectly mixed case data, proved to be inadequate in capturing the loss in biomass production observed in segregated bioreactors.

To sum up, it is possible to reproduce the experimental results using the IEM model with the same accuracy as spatially refined models. However, whatever the approach (spatial or statistical) it is necessary to increase the maintenance rate ( or reduce  $Y_{XG}$ ) in order to account for the effect of concentration heterogeneities on the substrate to biomass yield. These considerations led us to consider that the maintenance rate might increase with the heterogeneity of the glucose concentration field.

## 5.2. Changes in the maintenance rate

As stated in Section 3.2.1, substrate gradients may be responsible for the increased maintenance costs and, as seen in Tab.1 and in Tab.A.5,  $m$  is the parameter that is subject to the largest change with the degree of mixing. As proposed in Section 3.2.1, Eq.7 was implemented in the code obtaining an on-line calculation of the maintenance rate. The two constant in this law are identified as follows. The  $m_0$  value is set to 0.150  $mmol_G / g_X \cdot h$ , having hypothesized that in the

most homogeneous conditions (such as the *Case A* of the Neubauer et al. [16] experiment) this value represents a base level for  $m$ . Exploiting the data collected from the fed-batch simulations of the large scale fed-batch reactor, the variance of the substrate distribution was computed and its time averaged value used to set to  $\alpha = 4.86 \times 10^4 L^2 / g_X \cdot mmol_G \cdot h$  such that the resulting maintenance rate is  $\bar{m} = 0.250 mmol_G / g_X \cdot h$ . All the simulations were performed again, with the  $\bar{m}$  value linked to the degree of mixing in the bioactor and compared to those using a constant value, fitted for each case study. Results of the Xu et al. [44] experiment coupled with Eq.7 are shown in Fig.8.

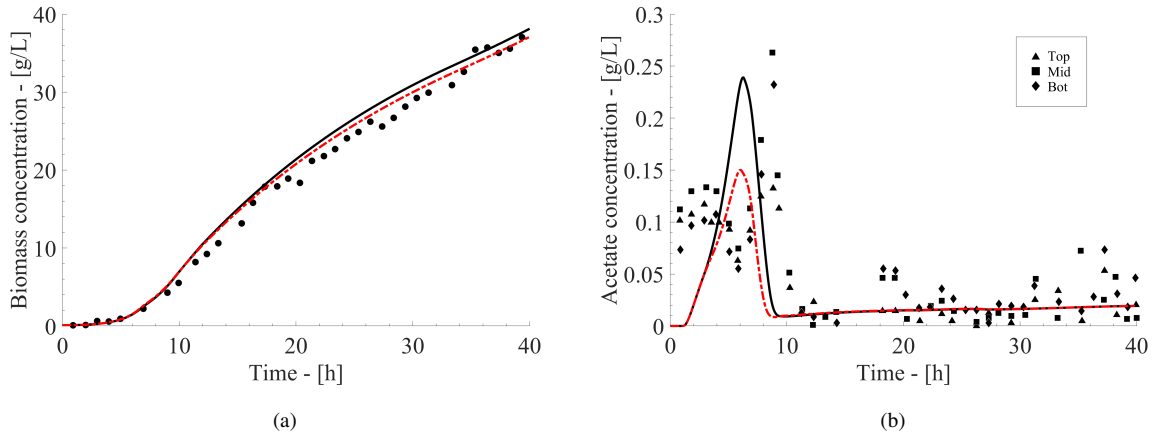


Figure 8: Average Biomass (a) and Acetate (b) concentration evolution in the Xu et al. [44] experiment. Experimental data (symbols) are collected at the top (*top*), middle (*mid*) and bottom (*bot*) of the fermenter. IEM model results are reported for simulations with constant (solid line) and variable (dashed line) maintenance rate.

Fig.8 shows that tying the local mean substrate concentration fluctuations to the maintenance rate does not produce substantial changes in the biomass concentration, shown in Fig.8a, where noticeable but small differences exist between the data obtained with a constant value of  $\bar{m}$  or with a variable  $\bar{m}$ . Fig.8b shows that different acetate profiles are obtained between about 3h and 9h from the beginning of the simulation. Before and after this time interval, the two acetate profiles obtained with constant and variable  $\bar{m}$  perfectly overlap. In particular, the simulation where the maintenance rate was allowed to change due to the substrate fluctuation produced a lower acetate concentration peak, due to a reduced fermentation rate. Indeed, Pigou and Morchain showed that substrate gradients develop from 7h onward as the substrate consumption characteristic time gets smaller than the mixing time [1]. The bioreactor is quite homogeneous up to 9h and the maintenance rate as predicted by Eq.7 is about  $0.150 mmol_G / g_X \cdot h$ , much lower than the value used for the constant maintenance rate simula-



tions ( $0.250 \text{ mmol}_G / \text{g}_X \cdot \text{h}$ ). Therefore less glucose is needed by the cells that find more oxygen to catabolize the substrate, resulting in less acetate production. The glucose concentration profiles as obtained with a constant and a variable value of maintenance rate are not shown since they almost perfectly overlap.

The benefit of using a variable maintenance rate is more obvious when simulating the Neubauer et al. [16] experiment, mainly because the cultivation consists in a batch (homogeneous) and a fed-batch (segregated) period of equal duration. The results are shown in Fig.9.

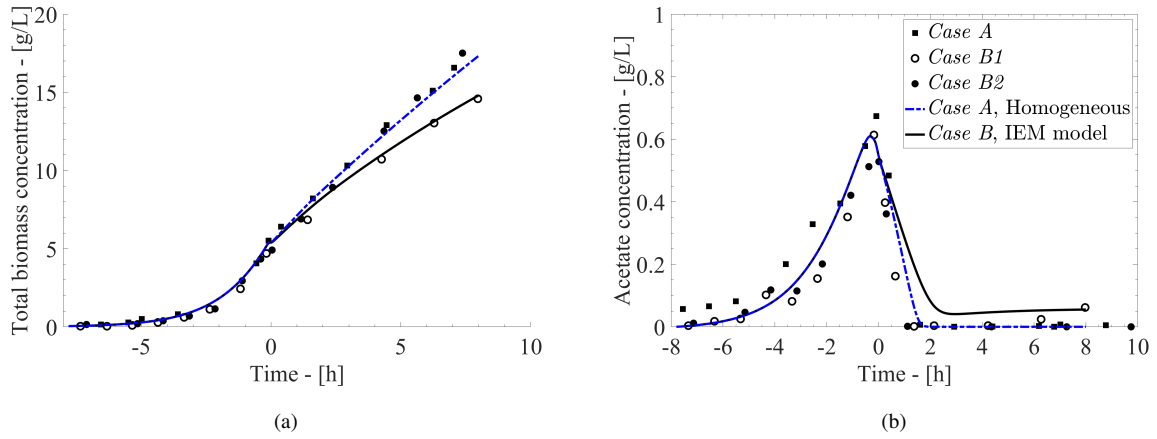


Figure 9: Total biomass (a) and Acetate (b) concentration evolution in the Neubauer et al. [16] experiment. Experimental data (symbols) and IEM model results obtained with variable  $\bar{m}$  for the Case A (dashed line) and B (solid line) experimental set-ups.

The biomass concentration profiles as obtained from the IEM model coupled with Eq.7 for the three different configurations described in Neubauer et al. [16] and the corresponding experimental data are shown in Fig.9a. The coupling of Eq.7 does not substantially affect the biomass concentration profiles of Case A. In fact, the high concentration feed plume is rapidly dispersed in the bulk of the STR, leading to  $\bar{m} \sim m_0 = \text{constant}$ . Considering the biomass concentration profile in Case B, the IEM model coupled with Eq.7 significantly improves the agreement between numerical and experimental results. In this case, the injection in the small plug flow reactor volume produces high local concentration peaks that are not promptly relieved. The acetate concentration profiles for the Cases A and B are shown in Fig.9b and no relevant differences are found with respect to the numerical simulations with constant maintenance rate. Also, with a variable maintenance rate, the residual acetate concentration is consistently predicted for the Case B, which is found in the Case B1 experiments as well.

## 6. Discussion

### 6.1. Time course of the maintenance rate

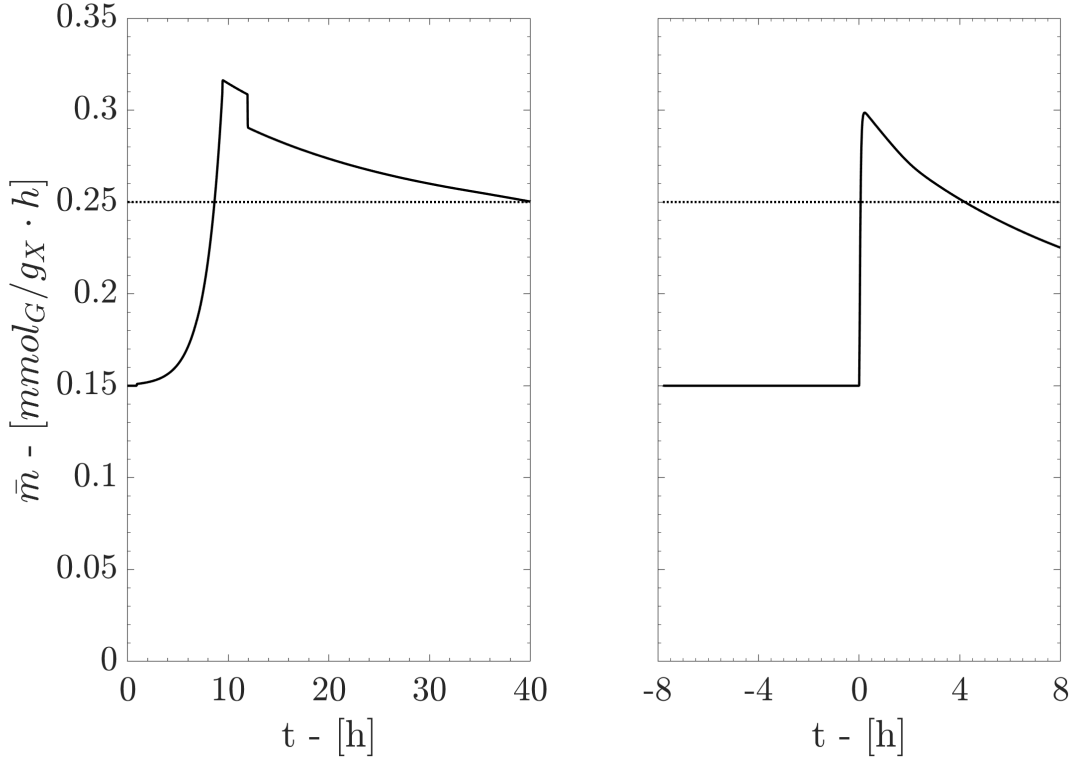


Figure 10:  $\bar{m}$ , solid line, as obtained from Eq.7 for the Xu et al. [44] experiment (on the left) and *Case B* of the Neubauer et al. [16] experiment (on the right). The dotted line represents a constant value of  $\bar{m} = 0.250 \text{ mmol}_G / g_X \cdot h$ .

In Fig.10, the evolution of  $\bar{m}$  in time is shown for the Xu et al. [44] and *Case B* of the Neubauer et al. [16] experiment. In the Xu et al. [44] experiment, on the left of Fig.10, assuming a constant value of  $\bar{m} = 0.250 \text{ mmol}_G / g_X \cdot h$  leads to an over-prediction of  $\bar{m}$  in the first  $\sim 9h$  of fermentation and a under-prediction of the mean maintenance rate in the last part of the process. Ultimately, the overall over- and under-predictions cancel out and considering  $\bar{m}$  constant and equal to  $\bar{m} = 0.250 \text{ mmol}_G / g_X \cdot h$  does not lead to substantial global differences. On the other hand,  $\bar{m}$  in *Case B* of the Neubauer et al. [16] experiment, on the right of Fig.10, exhibit two different behaviours. During the batch phase (negative times), the maintenance rate is constant and equal to its value at rest:  $\bar{m} = m_0 = 0.150 \text{ mmol}_G / g_X \cdot h$ . Right after the injection, high glucose inhomogeneities develop in the multistage reactor resulting in a sharp peak in the mean maintenance rate profile that is slowly relieved in the following part of the fermentation. Hy-

pothesizing a constant value of  $\bar{m} = 0.250 \text{ mmol}_G / g_X \cdot h$  leads to an important over-prediction of the maintenance cost in the batch phase that results in a lower biomass production during this phase. Conversely, during the fed batch phase, a constant  $\bar{m} = 0.250 \text{ mmol}_G / g_X \cdot h$  seems to be an acceptable fit, with an overall under- and over-prediction that, as in the Xu et al. [44] experiment, cancels out. On the other hand, hypothesizing a constant value of  $\bar{m} = 0.150 \text{ mmol}_G / g_X \cdot h$  works fine if the bioreactor is actually homogeneous ( *Case A* of the Neubauer et al. [16]), it also perfectly describes the batch phase but highly underestimates the mean maintenance cost, resulting in a higher final biomass production (as shown in Fig.7a). The very short batch phase in the Xu et al. [44] experiment results in an overall negligible effect of the over-estimation of the maintenance cost when considering a constant  $\bar{m} = 0.250 \text{ mmol}_G / g_X \cdot h$ , whereas, due to a longer batch phase, a single constant value for the batch and fed-batch phase proved to be inadequate in describing *Case B* of the Neubauer et al. [16] experiment.

The comparisons between the Xu et al. [44] and Neubauer et al. [16] experiments and the numerical simulations prove that disregarding the state of mixing and the inhomogeneities lead to inaccurate results, especially in terms of total biomass and acetate concentration. The results obtained with the IEM model closely match those obtained with the more accurate and more computational expensive compartment model, proving that the description of segregation with a simplified approach may be sufficient when the growth rate distribution is spatially invariant. An accurate biomass prediction heavily depends on the correct estimation of the glucose into biomass yield taking into account the increased maintenance due to concentration gradients. Further considerations on the metabolic response, such as overflow, are needed to account for the acetate production. However the metabolic responses leading to the formation of by-products can not, by themselves, explain the loss of biomass productivity evidenced in the experiments. Thus, gradients affect the cell on two different levels: the first order effect is the decreased yield and the second order effect is the production/consumption of acetate. A simple kinetic model using a variable yield given by equation 8 can suffice to account for the first effect whereas the addition of a metabolic model is needed to account for the by-product formation. Clearly, a vast, consistent and up-to-date data set, including gas phase measurements is needed to assess the generality of our proposition for a modified Pirt's law. The recent work of Anane et al. provides such a database [17].

## 6.2. Lagrangian formulation of the $\bar{m}$ model

Following a single cell in its path inside the bioreactor, it was hypothesized that the cell, subject to instantaneous and localized glucose fluctuations, changes its maintenance rate according to Eq.14, following the formulation proposed by Pigou [35] for the cell stresses.

$$\frac{dm}{dt} = \frac{K}{T_\sigma} \left( C_G(t) - \frac{1}{T_{bio}} \int_{t-T_{bio}}^t C_G(\tau) d\tau \right)^2 - \frac{m - m_0}{T_{rec}} \quad (14)$$

In Eq.14,  $C_G$ , refers to the instantaneous local concentration of glucose found by the cell along its path,  $K$  is a model constant representing the unit change in maintenance rate due to a unit change in the driving force (i.e. the squared concentration fluctuations),  $T_\sigma$  is a response time of the cell to external concentration fluctuations, the squared term in parenthesis represents the driving force of the change in the maintenance rate,  $m_0$  is the minimum maintenance rate of the cells and  $T_{rec}$  is a relaxation time toward the minimum maintenance rate  $m_0$ . The expression  $\frac{1}{T_{bio}} \int_{t-T_{bio}}^t C_G(\tau) d\tau$  is a time average of the concentrations previously encountered by the cell. This integral quantity is introduced to account for a memory effect, the fact that previously encountered concentrations contributed to set the present cell state (including its maintenance rate). It represents in some way an estimate of the concentration value to which the cell is accustomed. From that angle,  $T_{bio}$  can be interpreted as the time scale of long-term metabolic adaptation. The term in parenthesis therefore measures how much the local environment is different from the past conditions and thus be perceived as stressing from the cell point of view. In an homogeneous bioreactor, the time average is actually constant, equal to  $C_G$ , the environment is stress-less and the maintenance rate would relax toward the base level  $m_0$  with a dynamic defined by the characteristic time  $T_{rec}$ . In an heterogeneous bioreactor, the value of the time average concentration depends on the ratio between the mixing time and  $T_{bio}$ . If the mixing time is smaller than  $T_{bio}$ , the time average concentration can be regarded as the volume average  $\langle C_G \rangle$ .

In addition, changes in the maintenance rate are certainly much slower than the rate of change of substrate concentration along the cell trajectory, because the former is a consequence of the latter. Thus, in the limit of the derivative  $dm/dt$  being negligibly small, Eq.14 simplifies to:

$$m = m_0 + \alpha (C_G(t) - \langle C_G(t) \rangle)^2 \quad (15)$$

where the only parameter  $\alpha$ , already introduced in Eq.7, is equal to  $\frac{K \times T_{rec}}{T_\sigma}$ . Quite logically,  $\alpha$  results from the cell responsiveness, its response time and its recovery time to external fluctuations. As such, the cell based Lagrangian vision helps understanding the integral Eulerian model for  $\bar{m}$ .

A fruitful parallel can be made between equation Eq. 14, Eq. 4 and the metabolic model: in both cases a difference between the local conditions ( $\mu^*$  or  $C_G$ ) and a cell state variable ( $\mu$  or  $\int_{t-T_{bio}}^t C_G(\tau) d\tau$ ) is used to identify and quantify a cascade of biological responses. The short term metabolic response leading to overflow, the induced effects resulting in an increased maintenance rate and finally the long term response driving the population growth rate adaptation are accounted for at a minimal expense in terms of the number of internal cell variable.

In order to gain knowledge on the rate of change of maintenance rate for a population of cells, Eq.15 should be extended to a large number of particles. Ensemble averaging Eq.15 over the total number of cells in the reactor,  $N_{cells}$ , yields to:

$$\bar{m} = m_0 + \alpha \frac{1}{N_{cells}} \sum_{j=1}^{N_{cells}} \left( C_G^j - \langle C_G \rangle \right)^2 \quad (16)$$

where  $\bar{m}$  is the ensemble average maintenance rate and  $C_G^j$  is the substrate concentration along the trajectory of the  $j^{th}$  cell. Eq.7 is readily derived from Eq.16 since the number of cells in the reactor is large enough to sample the whole volume. The summation in Eq.16 is indeed a Monte Carlo calculation of the integral term in Eq.7

The parameters introduced in Eq.14 are a modeling choice aimed at describing in the most accurate way the different phenomena occurring in a cell subject to substrate concentration fluctuation, without adding constitutive equations for each of them. A comprehensive description of the effect of the substrate concentration fluctuations on the cell metabolism would require *ad hoc* experiments and insight on the single cell metabolic responses (such as in [11, 26, 48]), that is beyond the scope of this work. The modelling of the metabolic changes due to substrate concentration fluctuations put forward in this work has the goal to implement a simple Eulerian integral description for fast numerical simulations of heterogeneous bioreactors.

The single cell equation Eq.14 was solved for the Xu et al. [44] experiment and for Case B of the Neubauer et al. [16] experiments and, in both cases, it was hypothesized that the

cell spent a time exactly equal to  $\tau_{C_{S,max}}$  at higher substrate concentration and  $\tau_{C_{S,min}}$  at lower substrate concentration. Ideally, a distribution of residence time in the low concentration zone should be considered. The time trace of the glucose concentration experienced by these ideal cells is shown in Fig.11. Having divided the substrate concentration space in 70 sub-volumes and occurring the injection of fresh substrate in just one of the sub-volumes,  $\tau_{C_{S,max}}$  was assumed equal to  $\sim 3.6s$  for the Xu et al. [49] experiment, being this time equal to one seventieth of the macro-mixing time, and  $\tau_{C_{S,min}}$  equal to  $\sim 246.4s$ . In the numerical study concerning *Case B* of the Neubauer et al. [16] experiment,  $\tau_{C_{S,max}}$  was assumed equal to  $\tau_{PFR} = 113s$  and  $\tau_{C_{S,min}}$  equal to  $\tau_{STR} = 27min$ . The maximum,  $C_{S,max}$ , and minimum,  $C_{S,min}$  concentration in each simulation were assumed constant and equal to the whole-process-time average of the substrate concentration in the injection sub-volume(s) and in the remaining sub-volumes respectively. The time trace of the glucose concentration just introduced was used as  $C_G(t)$  in Eq.14 and the other constants are reported in Tab.3.

Table 3: Constants used in the solution of Eq.14.

Constant	Value	Units
$K$	$5 \times 10^3$	$L^2/g_X \cdot mmol_G \cdot h$
$T_\sigma$	$5 \times 10^{-4}$	$h$
$T_{bio}$	0.1	$h$
$m_0$	0.150	$mmol_G/g_X \cdot h$
$T_{rec}$	$5 \times 10^{-3}$	$h$

The characteristic time needed by the cell to adapt its metabolism to the substrate concentration in the surrounding environment,  $T_{bio}$ , was hypothesized to be long with respect to the other biological time scales as well as the fluid dynamics time scales. The values of the other constants should be determined from dedicated experiments, that is why, in this discussion, a systematic analysis of the constants of Eq.14 is overlooked. The constants  $K$ ,  $T_\sigma$  and  $T_{rec}$  and their ratio mostly influence the magnitude of the resulting  $\bar{m}$ . The constants were set in order to get  $\alpha = \frac{K \times T_{rec}}{T_\sigma}$  equal to  $5.00 \times 10^4 L^2/g_X \cdot mmol_G \cdot h$ , close to the value of  $\alpha = 4.86 \times 10^4 L^2/g_X \cdot mmol_G \cdot h$  identified through experiments in Section 5.2. The constant  $T_{bio}$  and especially the ratio between  $T_{bio}$  and the interval between two consecutive fluctua-

tions is what changes the overall integral behaviour of  $\bar{m}$ . The solution of Eq.14 for the two experiments is shown in Fig.11.

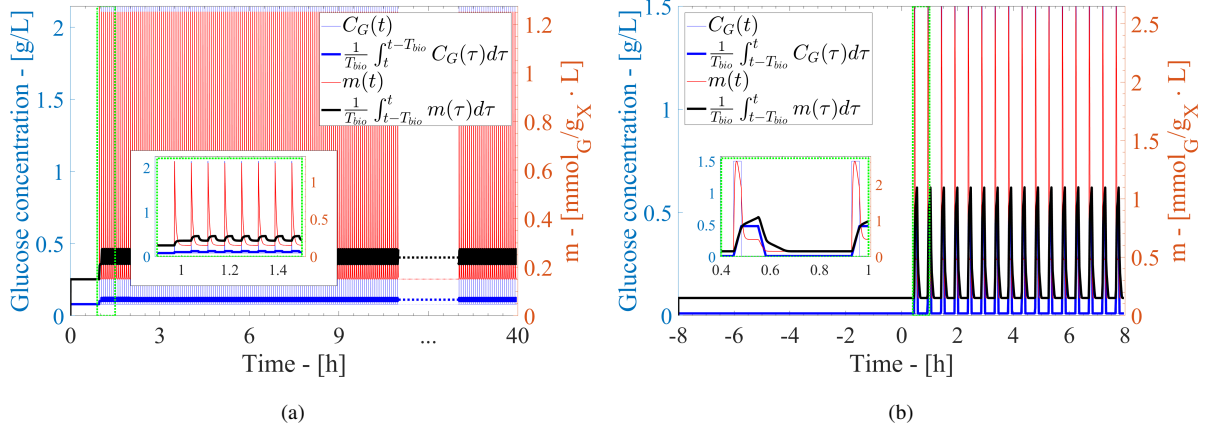


Figure 11: Instantaneous and averaged evolution of the glucose concentration experienced by the cells (left y-axis) and instantaneous and averaged maintenance rate (right y-axis). The simulations were devised to test the change in the maintenance rate due to substrate fluctuations for the Xu et al. [44] experiment (a) and for the Neubauer et al. [16] experiment (b).

From Fig.11a, in the zoomed drawing encircled with the dashed line, it is possible to see that the instantaneous maintenance rate obtained with the parameters in Tab.3 for the Xu et al. [44] experiment,  $m(t)$ , is subject to periodic peaks (due to the concentration fluctuations) after which it recovers its value at rest,  $m_0$ . Interestingly, the average  $m$  obtained over a  $T_{bio}$  time interval is almost constant during the fermentation, except for a short initial adjustment time immediately after the beginning of the fed-batch phase. As already mentioned, averaging in time over  $T_{bio}$  is equivalent to averaging over the volume or ensemble averaging over the entire microbial population. It is remarkable that the value of  $m$  is correctly predicted, owing to condition  $\alpha = \frac{KT_{rec}}{T_{\sigma}}$ . This indicates that our proposition to transform the Lagrangian dynamic model into an integral Eulerian expression is meaningful.

On the other hand, the zoomed drawing encircled with the dashed line in Fig.11b shows that in Case B of the Neubauer et al. [16] experiment the fluctuation characteristic time is longer with respect to Xu et al. [44]. In fact, the presence of the large STR with low substrate concentration adds a long residence time between two consecutive glucose fluctuations. During this time, the cells have time to adapt to the new low-concentration environment, producing metabolic changes that affect the instantaneous maintenance rate as well as its averaged value. When the cells are transported to the high glucose concentration environment the concentration

difference triggers a higher metabolic stress with respect to the previous case. This behavior is caught by the model in terms of time average glucose concentration (in thick blue line) that is almost constant in Fig.11a whereas it pulses due to the fluctuations in Fig.11b. Another important aspect is the duration of the concentration fluctuation that in *Case B* of the Neubauer et al. [16] experiment is two orders of magnitude larger than in the Xu et al. [44] experiment. This longer exposure to high concentration allows the cell to adjust to the new high concentration environment, allowing for a small  $m$  recovery in the high concentration environment. This single cell behaviour convoluted with the residence time distribution in the STR explains the increased maintenance at the population scale leading to a reduced production of biomass with respect to *Case A* of the same experiment.

### 6.3. Further considerations on the coupling with oxygen availability

In our simulations, the dissolved oxygen concentration is constant and equal to  $\sim 10\text{mg}_O/L$ , and fermentative metabolism could only take place because of a reduced oxygen uptake rate due to inhibition by acetate. Considering  $K_{i,A}^o = 4G_A/L$  along with residual acetate concentrations below  $10\text{mg}/L$  one can conclude that in absence of fermentation, the mixed acid metabolism is not responsible for the reduced yield. The reduction was entirely attributed to an increased maintenance rate as a results of gradient induced stresses. This corresponds to a possible explanation proposed in most studies mentioned in the introduction.

However, several authors also argued that an exposure to insufficient oxygen levels would trigger the mixed-acid fermentation pathways resulting in the production of lactate, formate and succinate from pyruvate. Thus, these pathways compete with the central metabolism pathway. Neubauer et al. [16] interpreted the reduced production of biomass in *Case B1* as a result of a suboptimal oxygen concentration inducing an acetate production through fermentation at the end of the PFR. To support this, they performed *Case B2* experiment (with enriched air injection in the PFR). The initial acetate production due to overflow metabolism was maintained but acetate formation due to fermentation was eliminated. Also, the production of biomass matches the biomass production in *Case A*. This result suggests that overflow, by itself, is not the main cause of yield reduction. Xu et al. repeated the experiments of Neubauer, confirming the previous results and finding that the various acids are re-assimilated almost entirely in the aerated STR. They explained that the repeated production and re-assimilation may be a contributing factor causing biomass loss upon scale-up [44]. Despite the fact that the oxygen sensor did not



reveal limiting levels in the  $20m^3$  experiments, they concluded that oxygen limitation is certainly present or perceived by the micro-organisms. In the end, mixed-acid fermentation lead to small amounts of by-products ( a few  $mg/L$ ) which can not quantitatively explain a decrease in biomass production of several  $g/L$ .

A possible explanation for this experimental observation is that the bacteria subject to intense substrate fluctuation almost instantaneously convert up to 30% of the substrate into  $CO_2$  with a specific uptake rate of  $O_2$  that was very similar to the specific rate of  $CO_2$  excretion [50]. This indicates that the oxygen demand increases as a result of over-assimilation. If enough oxygen is available, the massive excretion of  $CO_2$  limits the flood in the central metabolism and this mechanism therefore contributes to a reduction of the metabolic stresses, i.e. lower  $\bar{m}$  values. If the oxygen availability is insufficient (or the oxidative capacity of the cells is saturated) mixed-acid fermentation is triggered as well as a cascade of genetic and enzymatic bioprocesses which contribute to increasing the energetic *cost of living* from the cell point of view. It is therefore promising to consider that both substrate and oxygen distribution can contribute to a modification of the maintenance rate and extend the proposed approach to multiple nutrients.

## 7. Conclusions

In this work a two-environments IEM mixing model was implemented in the context of the software ADENON to describe the substrate inhomogeneities in two experimental fed-batch processes found in literature. Numerical simulations were performed to test how results obtained with the IEM model compared to numerical results obtained with a compartment model from literature and to the experimental results. A very good agreement was reached between the results obtained with the IEM and the compartment model, proving that a simplified description of the state of mixing could suffice when just substrate concentration spatial gradients are important. The agreement between the experimental and the numerical results is not worsened by the adoption of the simplified IEM model, in both the experimental set-ups found in literature. In comparison to other approaches (CFD and CMA), the use of an IEM model allow a fast and inexpensive simulation of highly segregated heterogeneous bioreactors. Considerations on the increase of the maintenance rate due to concentration fluctuations were necessary to improve the agreement with the experimental data. A modification to the Pirt's law introduc-

697 ing a dependence of the cell maintenance on the variance of the concentration distribution was  
698 hypothesized, validated against experimental data and discussed both from a Lagrangian and  
699 from an Eulerian perspective. This proposition constitutes a very simple and presumably gen-  
700 eral framework to connect concentration gradients to the maintenance rate. To sum up, the cost  
701 of living in an imperfectly mixed bioreactor increases with the variance of the concentration  
702 distribution.

## Appendix A. Sensitivity Analysis on the Neubauer experiment

A sensitivity study on the constants range highlighted that 6 constants of the metabolic model had the highest effects on the Neubauer et al. [16] results. The constants and their values can be found in Tab.A.4.

Table A.4: Model constants and their values used in the sensitivity study.

Constant	−30% (-1)	Xu et al. [44] value	+30% (+1)	Units
$\phi_O^{max}$	10.92	15.60	20.28	$mmol_O/g_X \cdot h$
$K_{i,A}$	2.10	3.00	3.90	$g_A/L$
$K_{i,A}^o$	2.80	4.00	5.20	$g_A/L$
$\bar{m}$	0.175	0.250	0.325	$mmol_G/g_X \cdot h$
$Y_{AG}$	2.10	3.00	3.90	$mol_A/mol_G$
$Y_{XG}^{max}$	0.92	1.32	1.72	$mol_X/mol_G$

A  $\pm 30\%$  deviation from the values proposed by Pigou and Morchain [1] to simulate the Xu et al. [44] experiment was studied, to map the sensitivity of the Neubauer et al. [16] results on the variations. Three response variables were observed, namely, the biomass concentration at the end of the fed-batch process, the maximum concentration of acetate found in the system during the whole process and the time needed to deplete the initial amount of glucose and therefore end the batch phase. The effects of the constants change on the response variables are shown in Fig.A.12, where the constant normalized values of  $\pm 1$  indicate a variation of  $\pm 30\%$  from the default values and the y-axis values are the percent change of the response variables with respect to the simulations with the default constants values (0).

Fig.A.12 shows that just a decrease in the maintenance rate,  $\bar{m}$ , or an increase in the maximum conversion yield of glucose in biomass,  $Y_{XG}^{max}$ , may lead to an increase of the final concentration of biomass. Both constants appear in the Pirt's formulation of the glucose to biomass conversion yield, Eq.6, but  $\bar{m}$  is related both to the bacteria and to the operating conditions, whereas  $Y_{XG}^{max}$  is presented as a maximum limit only dependent on the selected strain. Increasing the biomass concentration at the end of the fed-batch phase by changing the two constants presented above lead to a relatively large variation in the production of acetate, that can be adjusted with a variation of the other constants.

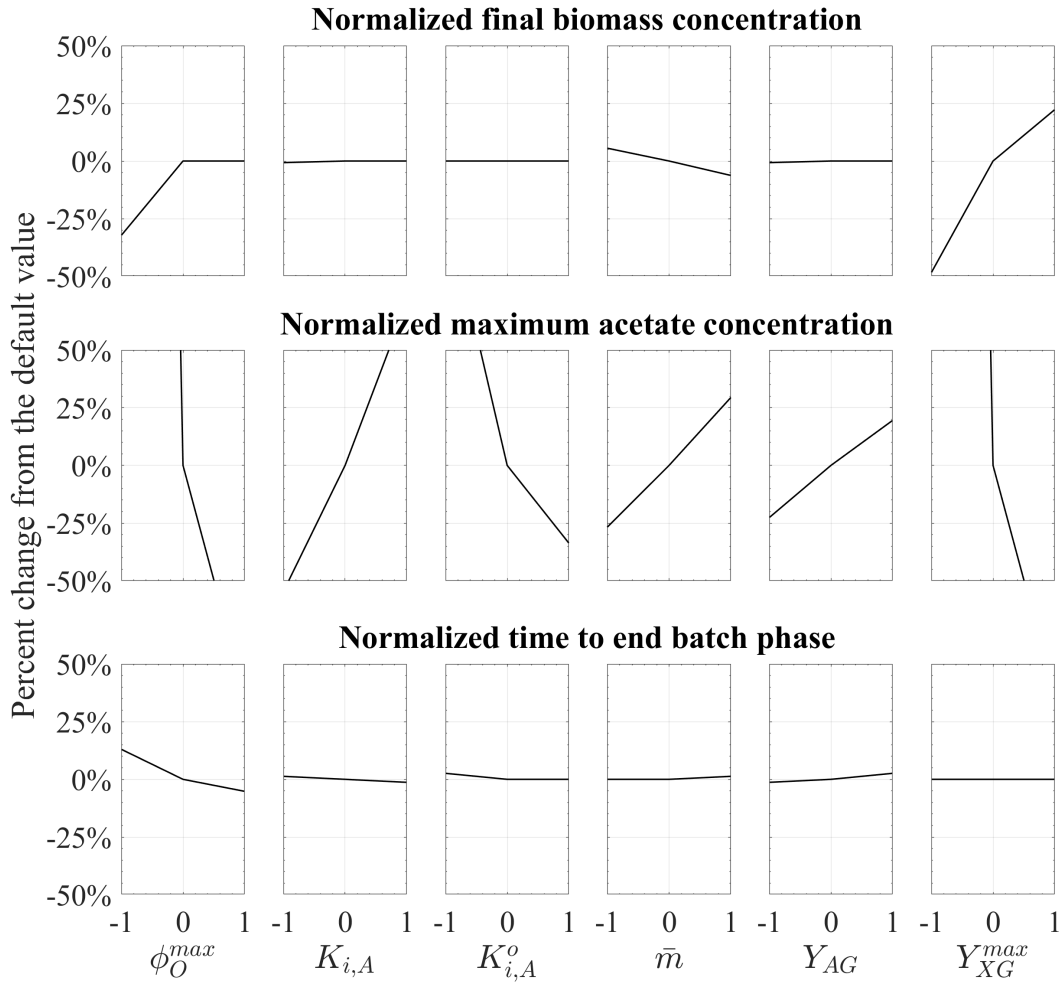


Figure A.12: Effect of the constants  $\pm 30\%$  variation on the response variables.

The sensitivity study was instrumental in tuning the constants in Tab.1 for the *Case A* of the Neubauer et al. [16] experiment. In Tab.A.5 the percent change of the constant values tuned for the Neubauer et al. [16] experiment with respect to the values proposed by Pigou and Morchain [1] to simulate the Xu et al. [44] experiment is reported. The constant values for the two experiments are reported in Tab.1.

Tab.A.5 shows that the maintenance rate is subject to the largest absolute value variation, pointing to the fact that a model to account for the change of  $\bar{m}$  in the two sets of experiments may be needed.

Table A.5: Model constants and their values used to improve the agreement with the *Case A* of the Neubauer et al. [16] experiment.

Constant	Percent change
$\phi_O^{max}$	−10.3%
$K_{i,A}$	+16.7%
$K_{i,A}^o$	0.0%
$\bar{m}$	−40.0%
$*Y_{AG}^{ferm}$	** −7.0%
$*Y_{AG}^{over}$	
$Y_{XG}^{max}$	+13.6%

\*\*The average  $Y_{AG}$  weighted on the acetate production mechanism is  $2.79 mol_A/mol_G$

## Appendix B. Further comments on model parameter identification

In section 5.2, the determination of  $\alpha$  is based on a fitting of experimental results.  $m_0 = 0.150 mmol_G/g_xh$  is obtained from experiments under homogeneous condition. When the reactor is heterogeneous and a constant maintenance rate is assumed, the latter has to be increased up to  $0.250 mmol_G/g_xh$ . It is proposed, in this work, to relate the maintenance rate to the variance of the concentration field. Therefore, the value of  $\alpha$  is fitted so that  $m(\sigma_C) = m_0 + \alpha(\sigma_C) = 0.250$ . The instantaneous variance,  $\sigma_C(t)$ , is obtained from the post-processing of spatially resolved simulations using a CMA approach and its time average value ( $\sigma_C$ ) is computed. This completely defines the value of  $\alpha$ .

In section 6.2, we provide an explanation for the formulation proposed in equation (7). For this, we consider several phenomena such as the cell responsiveness to concentration fluctuations,  $K$ , the time constant of that response  $T_\sigma$  and the recovery time constant  $T_{rec}$ . In the end, after some mathematical manipulations, it is shown that  $\alpha$  can be identified with the expression

$$\alpha = \frac{KT_\sigma}{T_{rec}} \quad (B.1)$$

And of course there is an infinity of triplet leading to the same value for  $\alpha$ . For that section however, we need to set a value for each parameter introduced. An arbitrary choice was made based on physical and biological considerations. We assumed that the response time  $T_\sigma$  is one order of magnitude larger than the recovery time  $T_{rec}$  (the opposite would lead to cells

749 being insensitive to external fluctuations). Then the response time should be shorter than the  
 750 exposure time which corresponds to the residence time in the concentrated zone (otherwise cells  
 751 would not perceive gradients). Looking at the concentration profile reported in the Neubauer  
 752 experiment (where  $\tau_{PFR} = 113s$ ), we can figure out that the response time to concentration  
 753 change is much shorter than the residence time in the PFR, thus we choose arbitrarily 2 seconds.  
 754 Then we get  $T_{rec} = 20s$  and since the targeted value for  $\alpha$  is known this sets the responsiveness  
 755 constant  $K$ . Because of that choice, the Lagrangian simulation in section 6.2 indicate that cells  
 756 seem to recover the stressing event in the Xu experiment because the residence time in the  
 757 stressing zone is much longer than in Neubauer's experiment. To sum up, in section 6.2, we  
 758 choose the parameter value quite arbitrarily (respecting some logical reasoning) in order to  
 759 enlighten the effects of the duration and frequency of concentration changes on the overall  
 760 maintenance rate. However, dynamic experiments such as those reported very recently by  
 761 Anane [17], performed massively on parallel bioreactor platforms, certainly provide enough  
 762 quantitative and informative data to perform a more precise parameter identification.

## References

- [1] M. Pigou, J. Morchain, [Investigating the interactions between physical and biological heterogeneities in bioreactors using compartment, population balance and metabolic models](#), Chemical Engineering Science 126 (2015) 267–282. doi:10.1016/j.ces.2014.11.035.  
URL <https://www.sciencedirect.com/science/article/pii/S0009250914006897https://linkinghub.elsevier.com/retrieve/pii/S0009250914006897>
- [2] G. S. Hansford, A. E. Humphrey, [The effect of equipment scale and degree of mixing on continuous fermentation yield at low dilution rates](#), Biotechnology and Bioengineering 8 (1) (1966) 85–96. doi:10.1002/bit.260080108.  
URL <http://doi.wiley.com/10.1002/bit.260080108>
- [3] E. H. Dunlop, S. J. Ye, [Micromixing in fermentors: Metabolic changes in \*Saccharomyces cerevisiae\* and their relationship to fluid turbulence](#), Biotechnology and Bioengineering 36 (8) (1990) 854–864. doi:10.1002/bit.260360816.  
URL <http://doi.wiley.com/10.1002/bit.260360816>
- [4] E. Plasari, R. David, J. Villiermaux, [Micromixing Phenomena in Continuous Stirred Reactors Using a Michaelis-Menten Reaction in the Liquid Phase](#), 1978, pp. 125–139. doi:10.1021/bk-1978-0065.ch011.  
URL <http://pubs.acs.org/doi/abs/10.1021/bk-1978-0065.ch011>
- [5] J. Bourne, F. Kozicki, P. Rys, [Mixing and fast chemical reaction—I](#), Chemical Engineering Science 36 (10) (1981) 1643–1648. doi:10.1016/0009-2509(81)80008-5.  
URL <https://www.sciencedirect.com/science/article/pii/0009250981800085https://linkinghub.elsevier.com/retrieve/pii/0009250981800085>
- [6] J. Baldyga, J. R. Bourne, [Interactions between mixing on various scales in stirred tank reactors](#), Chemical Engineering Science 47 (8) (1992) 1839–1848. doi:10.1016/0009-2509(92)80302-S.  
URL <https://www.sciencedirect.com/science/article/pii/000925099280302Shttps://linkinghub.elsevier.com/retrieve/pii/000925099280302S>
- [7] S. J. Ye, [Micromixing in \*Saccharomyces Cerevisiae\* aerobic fermentation](#), Ph.D. thesis, Washington University, Saint Louis, Missouri (1985).  
URL <http://crelonweb.eec.wustl.edu/theses/S.%20Ye.pdf>
- [8] S. O. Enfors, M. Jahic, A. Rozkov, B. Xu, M. Hecker, B. Jürgen, E. Krüger, T. Schweder, G. Hamer, D. O’Beirne, N. Noisommit-Rizzi, M. Reuss, L. Boone, C. Hewitt, C. McFarlane, A. Nienow, T. Kovacs, C. Trägårdh, L. Fuchs, J. Revstedt, P. C. Friberg, B. Hjertager, G. Blomsten, H. Skogman, S. Hjort, F. Hoeks, H. Y. Lin, P. Neubauer, R. van der Lans, K. Luyben, P. Vrabel, A. Manelius, [Physiological responses to mixing in large scale bioreactors.](#), Journal of biotechnology 85 (2) (2001) 175–85. doi:10.1016/S0168-1656(00)00365-5.  
URL <https://www.sciencedirect.com/science/article/pii/S0168165600003655http://www.ncbi.nlm.nih.gov/pubmed/11165362https://linkinghub.elsevier.com/retrieve/>

pii/S0168165600003655

- [9] R. Takors, Scale-up of microbial processes: Impacts, tools and open questions, *Journal of Biotechnology* 160 (1-2) (2012) 3–9. doi:10.1016/j.jbiotec.2011.12.010.  
URL <https://www.sciencedirect.com/science/article/pii/S0168165611006663>  
<https://linkinghub.elsevier.com/retrieve/pii/S0168165611006663>
- [10] A. Lemoine, N. Maya Martinez-Iturralde, R. Spann, P. Neubauer, S. Junne, Response of *Corynebacterium glutamicum* exposed to oscillating cultivation conditions in a two- and a novel three-compartment scale-down bioreactor, *Biotechnology and Bioengineering* 112 (6) (2015) 1220–1231. doi:10.1002/bit.25543.  
URL <http://doi.wiley.com/10.1002/bit.25543>
- [11] M. Löffler, J. D. Simen, J. Müller, G. Jäger, S. Laghrami, K. Schäferhoff, A. Freund, R. Takors, Switching between nitrogen and glucose limitation: Unraveling transcriptional dynamics in *Escherichia coli*, *Journal of Biotechnology* 258 (2017) 2–12. doi:10.1016/j.jbiotec.2017.04.011.  
URL <https://www.sciencedirect.com/science/article/pii/S0168165617301657>  
<https://linkinghub.elsevier.com/retrieve/pii/S0168165617301657>
- [12] P. Neubauer, S. Junne, Scale-down simulators for metabolic analysis of large-scale bioprocesses, *Current Opinion in Biotechnology* 21 (1) (2010) 114–121. doi:10.1016/j.copbio.2010.02.001.  
URL <https://www.sciencedirect.com/science/article/pii/S0958166910000157>  
<https://linkinghub.elsevier.com/retrieve/pii/S0958166910000157>
- [13] J. D. Fowler, E. H. Dunlop, Effect of reactant heterogeneity and mixing on catabolite repression in cultures of *Saccharomyces cerevisiae*, *Biotechnology and Bioengineering* 33 (1989) 1039–1046.
- [14] P. K. Namdev, B. G. Thompson, M. R. Gray, Effect of feed zone in fed-batch fermentations of *Saccharomyces cerevisiae*, *Biotechnology and Bioengineering* 40 (2) (1992) 235–246. doi:10.1002/bit.260400207.  
URL <http://doi.wiley.com/10.1002/bit.260400207>
- [15] S. George, G. Larsson, S. O. Enfors, A scale-down two-compartment reactor with controlled substrate oscillations: Metabolic response of *Saccharomyces cerevisiae*, *Bioprocess Engineering* 9 (6) (1993) 249–257. doi:10.1007/BF01061530.  
URL <http://link.springer.com/10.1007/BF01061530>
- [16] P. Neubauer, L. Haggström, S.-O. Enfors, Influence of substrate oscillations on acetate formation and growth yield in *Escherichia coli* glucose limited fed-batch cultivations, *Biotechnology and Bioengineering* 47 (2) (1995) 139–146. doi:10.1002/bit.260470204.  
URL <http://doi.wiley.com/10.1002/bit.260470204>
- [17] E. Anane, C. García, B. Haby, S. Hans, N. Krausch, M. Krewinkel, P. Hauptmann, P. Neubauer, M. N. Cruz Bournazou, A model-based framework for parallel scale-down fed-batch cultivations in mini-bioreactors for accelerated phenotyping, *Biotechnology and Bioengineering* 116 (11) (2019) 2906–2918. doi:10.1002/bit.27116.  
URL <https://doi.org/10.1002/bit.27116>



- [18] B. I. Tsai, L. E. Erickson, L. T. Fan, [The effect of micromixing on growth processes](#), *Biotechnology and Bioengineering* 11 (2) (1969) 181–205. doi:10.1002/bit.260110206.  
URL <http://doi.wiley.com/10.1002/bit.260110206>
- [19] L. T. Fan, B. I. Tsai, L. E. Erickson, [Simultaneous effect of macromixing and micromixing on growth processes](#), *AIChE Journal* 17 (3) (1971) 689–696. doi:10.1002/aic.690170336.  
URL <http://doi.wiley.com/10.1002/aic.690170336>
- [20] B. I. Tsai, L. T. Fan, L. E. Erickson, M. S. K. Chen, [The reversed two-environment model of micromixing and growth processes](#), *Journal of Applied Chemistry and Biotechnology* 21 (10) (1971) 307–312. doi:10.1002/jctb.5020211008.  
URL <http://doi.wiley.com/10.1002/jctb.5020211008>
- [21] R. K. Bajpai, M. Reuss, [Coupling of mixing and microbial kinetics for evaluating the performance of bioreactors](#), *The Canadian Journal of Chemical Engineering* 60 (3) (1982) 384–392. doi:10.1002/cjce.5450600308.  
URL <http://doi.wiley.com/10.1002/cjce.5450600308>
- [22] N. V. Mantzaris, J.-J. Liou, P. Daoutidis, F. Sreenc, [Numerical solution of a mass structured cell population balance model in an environment of changing substrate concentration](#), *Journal of Biotechnology* 71 (1-3) (1999) 157–174. doi:10.1016/S0168-1656(99)00020-6.  
URL <https://www.sciencedirect.com/science/article/pii/S0168165699000206https://linkinghub.elsevier.com/retrieve/pii/S0168165699000206>
- [23] M. A. Henson, [Dynamic modeling of microbial cell populations](#), *Current Opinion in Biotechnology* 14 (5) (2003) 460–467. doi:10.1016/S0958-1669(03)00104-6.  
URL <https://www.sciencedirect.com/science/article/pii/S0958166903001046https://linkinghub.elsevier.com/retrieve/pii/S0958166903001046>
- [24] J. Morchain, M. Pigou, N. Lebaz, [A population balance model for bioreactors combining interdivision time distributions and micromixing concepts](#), *Biochemical Engineering Journal* 126 (2017) 135–145. doi:10.1016/j.bej.2016.09.005.  
URL <https://www.sciencedirect.com/science/article/pii/S1369703X16302340https://linkinghub.elsevier.com/retrieve/pii/S1369703X16302340>
- [25] M. Stamatakis, [Cell population balance, ensemble and continuum modeling frameworks: Conditional equivalence and hybrid approaches](#), *Chemical Engineering Science* 65 (2) (2010) 1008–1015.  
URL <http://www.sciencedirect.com/science/article/pii/S00092509090006575>
- [26] A. Nieß, M. Löffler, J. D. Simen, R. Takors, [Repetitive Short-Term Stimuli Imposed in Poor Mixing Zones Induce Long-Term Adaptation of E. coli Cultures in Large-Scale Bioreactors: Experimental Evidence and Mathematical Model](#), *Frontiers in Microbiology* 8 (JUN) (2017) 1195. doi:10.3389/fmicb.2017.01195.  
URL <http://journal.frontiersin.org/article/10.3389/fmicb.2017.01195/full>
- [27] V. Quedeveille, H. Ouzaite, B. Polizzi, R. Fox, P. Villedieu, P. Fede, F. Létisse, J. Morchain, [A two-dimensional population balance model for cell growth including multiple uptake systems](#), *Chemical Engineering Research and Design* 132 (2018) 966–981. doi:10.1016/j.cherd.2018.02.025.

- URL <https://www.sciencedirect.com/science/article/pii/S026387621830090Xhttps://linkinghub.elsevier.com/retrieve/pii/S026387621830090X>
- [28] B. H. Hjertager, K. Morud, Computational fluid dynamics simulation of bioreactors, *Modeling, Identification and Control* 16 (4) (1995) 177–191. doi:10.4173/mic.1995.4.1.
- [29] S. Schmalzriedt, M. Jenne, K. Mauch, M. Reuss, *Integration of Physiology and Fluid Dynamics*, Springer Berlin Heidelberg, Berlin, Heidelberg, 2003, pp. 19–68. doi:10.1007/3-540-36782-9\_2.  
URL [https://doi.org/10.1007/3-540-36782-9\\_2](https://doi.org/10.1007/3-540-36782-9_2)
- [30] J. Morchain, J. C. Gabelle, A. Cockx, *Coupling of biokinetic and population balance models to account for biological heterogeneity in bioreactors*, *AIChE Journal* 59 (2) (2013) 369–379. doi:10.1002/aic.13820.  
URL <http://doi.wiley.com/10.1002/aic.13820>
- [31] P. Vrabel, R. G. Van der Lans, F. N. Van der Schot, K. C. A. Luyben, B. Xu, S. O. Enfors, *CMA: Integration of fluid dynamics and microbial kinetics in modelling of large-scale fermentations*, *Chemical Engineering Journal* 84 (3) (2001) 463–474. doi:10.1016/S1385-8947(00)00271-0.  
URL <https://www.sciencedirect.com/science/article/pii/S1385894700002710https://linkinghub.elsevier.com/retrieve/pii/S1385894700002710>
- [32] V. Alopaeus, P. Moilanen, M. Laakkonen, *Analysis of stirred tanks with two-zone models*, *AIChE Journal* 55 (10) (2009) 2545–2552. doi:10.1002/aic.11850.  
URL <http://dx.doi.org/10.1002/aic.11850>
- [33] A. Delafosse, M.-L. Collignon, S. Calvo, F. Delvigne, M. Crine, P. Thonart, D. Toye, *CFD-based compartment model for description of mixing in bioreactors*, *Chemical Engineering Science* 106 (0) (2014) 76–85. doi:10.1016/j.ces.2013.11.033.  
URL <http://www.sciencedirect.com/science/article/pii/S0009250913007690>
- [34] E. K. Nauha, Z. Kalal, J. M. Ali, V. Alopaeus, *Compartmental modeling of large stirred tank bioreactors with high gas volume fractions*, *Chemical Engineering Journal* 334 (2018) 2319–2334. doi:10.1016/j.cej.2017.11.182.  
URL <http://www.sciencedirect.com/science/article/pii/S1385894717321046>
- [35] M. Pigou, *Modelisation du comportement cinetique, des phenomenes de melange, de transfert locaux et des effets d’heterogeneite de population dans les fermenteurs industriels.*, *Genie des Procedes et de l’Environnement*, Universite de Toulouse, Institut National des Sciences Appliquees, Toulouse, France (Oct. 2018).
- [36] V. Gernigon, M. Chekroun, P. Guiraud, J. Morchain, *How Mixing and Light Heterogeneity Impact the overall Growth Rate in Photobioreactors*, *Chemical Engineering & Technology Under Review*.
- [37] C. Haringa, A. T. Deshmukh, R. F. Mudde, H. J. Noorman, *Euler-lagrange analysis towards representative down-scaling of a 22m<sup>3</sup> aerobic s. cerevisiae fermentation*, *13th International Conference on Gas-Liquid and Gas-Liquid-Solid Reactor Engineering* 170 (Supplement C) (2017) 653–669. doi:10.1016/j.ces.2017.01.014.  
URL <http://www.sciencedirect.com/science/article/pii/S0009250917300337>
- [38] F. Siebler, A. Lapin, M. Hermann, R. Takors, *The impact of co gradients on c. ljungdahlia in a 125m<sup>3</sup> bubble*

- column: Mass transfer, circulation time and lifeline analysis, *Chemical Engineering Science* 207 (2019) 410–423. doi:10.1016/j.ces.2019.06.018.
- URL <http://www.sciencedirect.com/science/article/pii/S0009250919305159>
- [39] J. Villermaux, J. Devillon, Représentation de la coalescence et de la redispersion des domaines de ségrégation dans un fluide par un modèle d’interaction phénoménologique, in: *Proceedings of the 2nd International symposium on chemical reaction engineering*, 1972, pp. 1–13.
- [40] J. Morchain, *Bioreactor Modeling : Interactions between Hydrodynamics and Biology.*, ISTE Press Ltd/Elsevier Ltd, London/Oxford, 2017.
- URL [https://books.google.ca/books?hl=en&lr=&id=-w4TDgAAQBAJ&oi=fnd&pg=PP1&dq={%}22bioreactor+modeling{%}22+morchain&ots=9if\\_{\\_}q\\_{\\_}CCmQa{&sig=tran3Vbx1rvQzoKFPxLPonBbb8E{#}v=onepage{&q={%}22bioreactormodeling{%}22morchain{&f=false](https://books.google.ca/books?hl=en&lr=&id=-w4TDgAAQBAJ&oi=fnd&pg=PP1&dq={%}22bioreactor+modeling{%}22+morchain&ots=9if_{_}q_{_}CCmQa{&sig=tran3Vbx1rvQzoKFPxLPonBbb8E{#}v=onepage{&q={%}22bioreactormodeling{%}22morchain{&f=false)
- [41] S. Pirt, The maintenance energy of bacteria in growing cultures, *Proceedings of the Royal Society of London. Series B. Biological Sciences* 163 (991) (1965) 224–231. doi:10.1098/rspb.1965.0069.
- URL <http://www.royalsocietypublishing.org/doi/10.1098/rspb.1965.0069>
- [42] H. Holms, Flux analysis and control of the central metabolic pathways in *Escherichia coli*, *FEMS Microbiology Reviews* 19 (2) (1996) 85–116. doi:10.1016/S0168-6445(96)00026-5.
- URL <https://academic.oup.com/femsre/article-lookup/doi/10.1111/j.1574-6976.1996.tb00255.xhttp://linkinghub.elsevier.com/retrieve/pii/S0168644596000265>
- [43] A. L. Meadows, R. Karnik, H. Lam, S. Forestell, B. Snedecor, Application of dynamic flux balance analysis to an industrial *Escherichia coli* fermentation, *Metabolic Engineering* 12 (2) (2010) 150–160. doi:10.1016/j.ymben.2009.07.006.
- URL <https://www.sciencedirect.com/science/article/pii/S1096717609000627https://linkinghub.elsevier.com/retrieve/pii/S1096717609000627>
- [44] B. Xu, M. Jahic, G. Blomsten, S.-O. Enfors, Glucose overflow metabolism and mixed-acid fermentation in aerobic large-scale fed-batch processes with *Escherichia coli*, *Applied Microbiology and Biotechnology* 51 (5) (1999) 564–571. doi:10.1007/s002530051433.
- URL <https://link-springer-com.ezproxy.unibo.it/content/pdf/10.1007/{%}2Fs002530051433.pdfhttp://www.ncbi.nlm.nih.gov/pubmed/10390814http://link.springer.com/10.1007/s002530051433>
- [45] J. Morchain, J. C. Gabelle, A. Cockx, A coupled population balance model and CFD approach for the simulation of mixing issues in lab-scale and industrial bioreactors, *AIChE Journal* 60 (1) (2014) 27–40. doi:10.1002/aic.14238.
- URL <http://doi.wiley.com/10.1002/aic.14238>
- [46] J. Morchain, C. Fonade, A structured model for the simulation of bioreactors under transient conditions, *AIChE Journal* 55 (11) (2009) 2973–2984. doi:10.1002/aic.11906.
- URL <http://dx.doi.org/10.1002/aic.11906>
- [47] R. O. Fox, *Computational Models for Turbulent Reacting Flows*, Cambridge University Press, Cambridge,

2003. doi:10.1017/CB09780511610103.

URL <http://cds.cern.ch/record/997036http://ebooks.cambridge.org/ref/id/CB09780511610103>

- [48] J. D. Simen, M. Löffler, G. Jäger, K. Schäferhoff, A. Freund, J. Matthes, J. Müller, R. Takors, Recog-  
Nice Team, R. Feuer, J. von Wulffen, J. Lischke, M. Ederer, D. Knies, S. Kunz, O. Sawodny, O. Riess,  
G. Sprenger, N. Trachtmann, A. Nieß, A. Broicher, [Transcriptional response of Escherichia coli to ammonia  
and glucose fluctuations](#), Microbial Biotechnology 10 (4) (2017) 858–872. doi:10.1111/1751-7915.  
12713.

URL <http://www.ncbi.nlm.nih.gov/pmc/articles/PMC5481515/>

- [49] B. Xu, M. Jahic, S. O. Enfors, [Modeling of overflow metabolism in batch and fed-batch cultures of Es-  
cherichia coli](#), Biotechnology Progress 15 (1) (1999) 81–90. doi:10.1021/bp9801087.

URL <http://doi.wiley.com/10.1021/bp9801087>

- [50] S. Sunya, F. Delvigne, J.-L. Uribelarra, C. Molina-Jouve, N. Gorret, Comparison of the transient responses  
of Escherichia coli to a glucose pulse of various intensities, Applied Microbiology And Biotechnology 95 (4)  
(2012) 1021–1034.